



**An-Najah National University**  
**Faculty of Graduate Studies**

**STRUCTURAL, ELECTRONIC, MAGNETIC,  
AND ELASTIC PROPERTIES OF THE FULL-  
HEUSLER COMPOUNDS:  $\text{Sc}_2\text{ZrAl}$ ,  $\text{Sc}_2\text{ZrIn}$   
USING FP-LAPW METHOD**

**By**

**Ruba Zahi Theeb Al-Gharabah**

**Supervisors**

**Dr. Mahmoud Farout**

**Prof. Mohammed Abu-Jafar**

**This Thesis is Submitted in Partial Fulfillment of the Requirements for the Degree of  
Master of Physics, Faculty of Graduate Studies, An-Najah National University,  
Nablus - Palestine.**

**2024**

# **STRUCTURAL, ELECTRONIC, MAGNETIC, AND ELASTIC PROPERTIES OF THE FULL-HEUSLER COMPOUNDS: $\text{Sc}_2\text{ZrAl}$ , $\text{Sc}_2\text{ZrIn}$ USING FP-LAPW METHOD**

By

Ruba Zahi Theeb Al-Gharabah

This Thesis was Defended Successfully on 26/6/2024 and approved by:

Dr. Mahmoud Farout  
Supervisor

Prof. Mohammed Abu-Jafar  
Co-Supervisor

Prof. Jihad Asad  
External Examiner

Dr. Musa Al-Hasan  
Internal Examiner



Signature

Signature

Signature

Signature

## **Dedication**

To the one who bet on my success from a young age to the soul of my dear grandfather, " Abu Ali", may God have mercy on him...

To my role model, my support in life, who proudly attached his name to mine, my dear father, whose encourage guides me through my master journey. Your belief in me has shaped me into the person I am today...

To my angel in life, her prayers are the secret of my success, my beautiful, my dear mother...

To those who share all the moments of my life with me, partners in childhood and youth, my dear brothers...

To the one whose unweaving emotional and intellectual support guided me through this thesis, your encouragement has been instrumental in this academic endeavor, my dear partner...

To everyone who taught me a letter and everyone who encouraged me to achieve this success.

## **Acknowledgments**

Praise and thanks be to God who inspired me to complete postgraduate studies, and then I extend my sincere thanks to my research supervisors, Dr. Mahmoud Farout and Prof Dr. Mohammed Abu-Jafar, who did not spare a moment of time and information to help me accomplish this work, and advised me in every step, may God protect them. To all the staff in the Physics Department, from whom we learned, who provide us with knowledge and benefit, the treasure of knowledge. To everyone who helped me complete this work... Thanks from the heart.

## Declaration

I, the undersigned, declare that I submitted the thesis entitled:

**STRUCTURAL, ELECTRONIC, MAGNETIC, AND ELASTIC PROPERTIES OF THE FULL-HEUSLER COMPOUNDS:  $\text{Sc}_2\text{ZrAl}$ ,  $\text{Sc}_2\text{ZrIn}$  USING FP-LAPW METHOD**

I declare that the work provided in this thesis, unless otherwise referenced, is the researcher's own work, and has not been submitted elsewhere for any other degree or qualification.

Student's Name: Ruba Zahi Al-gharobah.

Signature: Ruba Z. Ghawabeh

Date: 26-6-2024

## List of Contents

|  |      |
|--|------|
| Dedication .....   | III  |
| Acknowledgments .....                                      | IV   |
| Declaration.....   | V    |
| List of Contents.....                                      | VI   |
| List of Tables .....                                       | VIII |
| List of Figures .....                                      | IX   |
| List of Appendices .....                                   | X    |
| Abstract.....  | XII  |
| Chapter one: Introduction .....                            | 1    |
| 1.1 Background.....  | 1    |
| 1.3 Study Gap .....  | 7    |
| 1.4 Literature Review .....                                | 8    |
| 1.5 Importance of this thesis .....                        | 14   |
| Chapter Two: Methodology.....                              | 16   |
| 2.1 The Born-Oppenheimer Approximation (BOA).....          | 17   |
| 2.2 Hartree and Hartree-Fock Approximation.....            | 18   |
| 2.3 Density Functional Theory (DFT) .....                  | 19   |
| 2.4 Single particle Kohn-Sham Equation .....               | 21   |
| 2.5 The Exchange-Correlation Functional.....               | 23   |
| 2.6 Local Density Approximation (LDA).....                 | 24   |
| 2.7 Generalized Gradient Approximation (GGA) .....         | 25   |
| 2.8 Augmented Plane Wave (APW) Method.....                 | 26   |
| 2.9 The Linearized Augmented Plane Wave (LAPW) Method..... | 27   |
| 2.10 Modified Becke-Johnson Potential (mBJ).....           | 28   |
| Chapter Three: Results.....                                | 30   |
| 3.1 General look on WIEN2k .....                           | 30   |
| 3.2 WIE2k techniques.....                                  | 31   |
| 3.3 Structural Properties .....                            | 33   |
| 3.4 Magnetic Properties .....                              | 38   |
| 3.5 Electronic Properties.....                             | 41   |
| 3.6 Elastic properties.....                                | 46   |
| Chapter Four: Discussions and Conclusions .....            | 51   |

|                             |    |
|-----------------------------|----|
| List of Abbreviations ..... | 53 |
| References.....             | 54 |
| Appendices.....             | 61 |
| الملخص.....                 | ب  |

## List of Tables

|   |    |
|---|----|
| Table 1: Theoretical values from yilin Han et al study.....   | 7  |
| Table 2: The lattice parameter (a), bulk modulus (B), its first derivative (B) and the minimum energy ( $E_0$ ) .....   | 38 |
| Table 3: Total, partial magnetic moment for inverse and normal $Sc_2ZrAl$ and $Sc_2ZrIn$ <sup>(45)</sup> .....  | 40 |
| Table 4: Energy band gap of normal and inverse of $Sc_2ZrAl$ , and $Sc_2ZrIn$ utilizing PBE-GGA and mBJ potentials .....  | 42 |
| Table 5: The elastic constants ( $C_{ij}$ ), bulk modulus (B), and anisotropic factor (A) of $Sc_2ZrAl$ and $Sc_2ZrIn$ .....  | 49 |
| Table 6: Bulk modulus (B), Shear modulus (S), B/S ratio, Voigt Poisson's ratio ( $\nu$ ), and Young's modulus (Y) of normal $Sc_2ZrAl$ and normal $Sc_2ZrIn$ compounds .... | 49 |

## List of Figures

|  |    |
|--|----|
| Figure 1: Elements forming Heusler alloys $X_2YZ$ .....  | 6  |
| Figure 2: The scheme for the nth relationship in the self-consistent steps to clarify Hartree-Fock or Kohn-Sham equations.....   | 23 |
| Figure 3: Scheme of Augmented Plane Wave .....   | 26 |
| Figure 4: Crystal structures of $Sc_2ZrAl$ and $Sc_2ZrIn$ in (a) normal Heusler ( $L2_1$ ) and (b) inverse Heusler ( $Xa$ ) (Red: Sc, Green: Zr, Blue: Al/In).....                   | 35 |
| Figure 5: The overall energy (Ry) versus volume ( $a.u^3$ ) for both normal $Sc_2ZrAl$ Heusler and inverse $Sc_2ZrAl$ Heusler.....   | 36 |
| Figure 6: The overall energy (Ry) versus volume ( $a.u^3$ ) for normal $Sc_2ZrIn$ Heusler and inverse $Sc_2ZrIn$ Heusler .....   | 37 |
| Figure 7: The band structure for normal $Sc_2ZrAl$ Heusler compound by employing PBE-GGA method for (a) spin down normal Heusler compound, (b) spin up normal Heusler compound. .... | 42 |
| Figure 8: The band structure for inverse $Sc_2ZrAl$ Heusler compound by using PBE-GGA method for (a) spin down inverse Heusler compound (b) spin up inverse Heusler compound.....    | 43 |
| Figure 9: The band structure for normal $Sc_2ZrAl$ Heusler compound by using mBJ-GGA method for (a) spin down normal Heusler compound (b) spin up normal Heusler compound.....       | 44 |
| Figure 10: The band structure for inverse $Sc_2ZrAl$ Heusler compound by using mbj method for (a) spin down regular Heusler compound (b) spin up regular Heusler compound.....       | 45 |

## List of Appendices

|   |    |
|---|----|
| Appendix A: Figures of Study .....  | 61 |
| Figure 11: The band structure for normal $\text{Sc}_2\text{ZrIn}$ Heusler compound by using GGA method for (a) spin down normal Heusler compound (b) spin up normal Heusler compound .....  | 61 |
| Figure 12: The band structure for inverse $\text{Sc}_2\text{ZrIn}$ Heusler compound by using GGA method for (a) spin down regular Heusler compound (b) spin up regular Heusler compound .....   | 62 |
| Figure 13: The band structure for normal $\text{Sc}_2\text{ZrIn}$ Heusler compound by using mBJ method for (a) spin down normal Heusler compound, (b) spin up normal Heusler compound .....   | 63 |
| Figure 14: The band structure for inverse $\text{Sc}_2\text{ZrIn}$ Heusler compound by using mBJ method for (a) spin down normal Heusler compound, (b) spin up normal Heusler compound .....  | 64 |
| Figure 15: (a) Total density of states of spin up and spin down for normal $\text{Sc}_2\text{ZrAl}$ and partial density of states of spin up and spin down for (b) Sc atom (c) Zr atom (d) Al atom of normal compound using GGA method .....                | 65 |
| Figure 16: (a) Total density of states of spin up and spin down for normal $\text{Sc}_2\text{ZrAl}$ and partial density of states of spin up and spin down for (b) Sc atom (c) Zr atom (d) Al atom of normal compound using mBJ method .....                | 66 |
| Figure 17: (a) Total density of states of spin up and spin down for inverse $\text{Sc}_2\text{ZrAl}$ and partial density of states of spin up and spin down for (b) Sc1 atom (c) Sc2 atom (d) Zr atom (e) Al atom of inverse compound using GGA method....  | 67 |
| Figure 18: (a) Total density of states of spin up and spin down for inverse $\text{Sc}_2\text{ZrAl}$ and partial density of states of spin up and spin down for (b) Sc1 atom (c) Sc2 atom (d) Zr atom (e) Al atom of normal compound using mBJ method ..... | 68 |
| Figure 19: (a) Total density of states of spin up and spin down for normal $\text{Sc}_2\text{ZrIn}$ and partial density of states of spin up and spin down for (b) Sc atom (c) Zr atom (d) In atom of normal compound using GGA method.....                 | 69 |
| Figure 20: (a) Total density of states of spin up and spin down for normal $\text{Sc}_2\text{ZrIn}$ and partial density of states of spin up and spin down for (b) Sc atom (c) Zr atom (d) In atom of normal compound using mBJ method .....                | 70 |

Figure 21: (a) Total density of states of spin up and spin down for inverse  $\text{Sc}_2\text{ZrIn}$  and partial density of states of spin up and spin down for (b) Sc1 atom (c) Sc2 atom (d) Zr atom (e) In atom of inverse compound using GGA method .... 71

Figure 22: (a) Total density of states of spin up and spin down for inverse  $\text{Sc}_2\text{ZrIn}$  and partial density of states of spin up and spin down for (b) Sc1 atom (c) Sc2 atom (d) Zr atom (e) In atom of inverse compound using mBJ method..... 72

**STRUCTURAL, ELECTRONIC, MAGNETIC, AND ELASTIC PROPERTIES  
OF THE FULL-HEUSLER COMPOUNDS:  $\text{Sc}_2\text{ZrAl}$ ,  $\text{Sc}_2\text{ZrIn}$  USING  
FP-LAPW METHOD**

**By**

**Ruba Zahi Theeb Al-Gharabah**

**Supervisors**

**Dr. Mahmoud Farout**

**Prof. Mohammed Abu-Jafar**

**Abstract**

Structural, electronic, elastic, and magnetic properties of the Full-Heusler Compounds:  $\text{Sc}_2\text{ZrAl}$ ,  $\text{Sc}_2\text{ZrIn}$  have been investigated and examined by utilizing full potential linearized augmented plane wave method (FP-LAPW). This method provides more accurate estimations of the electronic structure of atoms. We have used the Density Functional Theory (DFT), which is a computational quantum mechanical modelling method being implemented in the WIEN2k package. FP-LAPW method is an application of Kohn-Sham (DFT), which typically goes with the study of core and valence electrons, the ground state density, total energy, and Kohn-Sham eigenvalues (energy bands) of a many-electron system. Structural parameters (bulk modulus, lattice parameters and first pressure derivatives) have been investigated by applying the generalized gradient approximation (PBE-GGA). Also, the modified Becke-Johnson (mBJ) was used computationally to develop and enhance the calculated value of energy band gap for these compounds. Mechanically, we identified that the normal full-Heusler compounds  $\text{Sc}_2\text{ZrAl}$  and  $\text{Sc}_2\text{ZrIn}$  were stable, while the inverse full-Heusler compounds  $\text{Sc}_2\text{ZrAl}$  and  $\text{Sc}_2\text{ZrIn}$  were unstable. This result agrees with previous studies.

**Keywords:** Heusler compounds; Full Heusler compounds; Generalized gradient approximation; Modified Becke Johnson; Local density function; Magnetic moment.

# Chapter one

## Introduction

### 1.1 Background

In Germany, an engineer and chemist scientist called “Friedrich Heusler” (1866- 1947), he awarded his Ph.D in 1887 from the university of Berlin. After studying, he worked in several fields, first at the university where he studied, then he was qualified and had his own business. In 1901, he started working with some compounds to study their properties, he discovered some ferromagnetic intermetallic compounds, which was called “Heusler compounds” and the term Heusler derives and come from his name. <sup>(1)</sup>

The shock was some compounds are ferromagnetic though none of their components are ferromagnetic. Ferromagnetic materials mean materials which present intense magnetic properties. Popularly this property happens in transition metals such as: iron, cobalt, and nickel, as well as the alloys of these metals.

Ferromagnetic materials are widely used in many applications like sensors, data storage, and because of their ability in holding over their magnetization they are commonly applied in electric motors.

In 1903, Heusler conducted groundbreaking investigations and studied the compound  $\text{Cu}_2\text{MnAl}$ . Peculiarly, this alloy was ferromagnetic, despite the absence of magnetic properties in its components.

Relatively, for a long time the origin of ferromagnetic behavior wasn't explained. Heusler explained the reason of that is because of the addition of some elements with *sp* configuration such as (Indium (In), Aluminum (Al), Tin (Sn), Strontium (Sb) or Bismuth (Bi)). These elements turn the alloy and make it a ferromagnetic material.

The Manganese (Mn) element, with atomic number equals 25. Which is located at the body centers of the cubic structure, was the reason that made the first Heusler alloy to be ferromagnetic. Also, Mn was the key to unlocking the magnetic properties in this compound. <sup>(1)</sup>

Moreover, it was discovered that not just this alloy, but also a whole collection of alloys have the same behavior. Nowadays, the exploration of Heusler alloys with researchers, more than a thousand Heusler alloys are known.

For determining the magnetic properties, crystal structure, composition and heat treatment were found very important parameters. This topic has a great importance in the classification of materials depending on various behavior of spin-up and spin-down bands. This indicates to the energy band, which is created by electrons according to electron spin orientation.

When the electrons are with spin-up bands, the spin is in one direction, they show metallic attitude. While electrons with spin-down bands, the spin is in the opposite direction, they show semiconductors behavior, the material is classified as a half metal.

The metals are distinguished by their high ability to conduct electricity, and heat as well as their ductile nature. Metals are materials with a lot of free electrons most of them with parallel spin, causing total magnetic moment.

Half metal materials are materials that show metallic behavior for one orientation, and show semiconductor or insulating behavior for the different orientation of spin. So they have automatic and immediate total magnetic moment, which means they are commonly ferromagnetic materials.

In addition, we can classify and assort the materials into metallic, semiconductors, semimetals and other many various types depending on their magnetic order like ferromagnetic, antiferromagnetic and half metallic ferromagnetic.

Semimetals pointing to the materials with properties in the midst of metals and semiconductors, such as: Si, and Ge which are broadly implemented in semiconductor devices. In semimetals the conduction band is filled partially. While the valence band is empty.

Heusler compounds have special featured and distinguished properties in addition to the excellent controllability, the controllability of materials means a magnetic function which is used to get more accuracy.

Heusler compounds exhibit a plethora of interesting physical characteristics. Which, in turn, contributed to make these compounds have garnered widespread attention and greatly dominate in numerous applications in many fields, among the most famous examples of these applications that basically based on this topic: spintronic, which is related to the first discoveries in 1980s.

Since Heusler compounds play a critical role in developing spin-based electronic devices, there are many applications depend in turn on the study of Heusler compounds. Heusler compounds are applied in thermoelectric materials, which is a type of materials that can converge the thermal energy into electrical energy, by the transport of charge and heat. The carriers in this method are electrons and phonons.

Additionally, Heusler compounds are rendered as a foundation for the spin-gapless semiconductors (SGSs). The (SGSs) materials are ones with no band gap in one channel from the other spin channels, but on the other spin channels the gap is finite. This property in turn offers many promising opportunities for spin-polarized electronic applications.

Heusler compounds participate in the advancement of topological insulators, materials with specific electron properties that make them insulate inside in their bulk, since the electrons are not moving spontaneously and conducting electricity along the surface or edge, due to the electrons freely motion.

In addition they have applications in shape memory alloys (SMAs) allowing for reversible deformation under some specific conditions, and superconductors, which exhibit extraordinary conducting properties. (SMAs) are metallic materials can regain to the original shape after deformation. So (SMAs) are widely used in many features such as: robotics, aerospace, and medical devices

Moreover they are used in manufacturing magnetic memory devices, which use a magnetic storage in order to hold and preserve information. As well as some Heusler compounds are widely used as catalyst in chemical reactions like oxidation.

Heusler compounds have stood out as an important, decisive, and critical opponent in the material science domain, by showing off and boasting several distinct applications as mentioned above.

## 1.2 Structure of Heusler alloys

Heusler alloys are an enormous number of compounds with intermetallic components with over 1000, -about 1500- members with a wide range of different properties. These properties depend on an important factor which is the valence electron's number, valence electrons means the electrons located in the outermost shell of the atom.

Valence electrons can determine the alloy's properties such as: band gaps, magnetic, electrical properties, and chemical bonds between atoms, since the valence electrons determine if the atom tends to lose, gain, or share electrons. The structure of Heusler alloys beside its intricacies and complexity it renders as the cornerstone in understanding the properties, behavior and applications of Heusler compounds. In addition to its turn in determining their electronic, structural, magnetic and elastic properties.

Heusler compounds usually includes three elements with a particular structure, their structure varies between many types, such as: cubic, tetragonal, and hexagonal arrangements.

Studying the structure of Heusler alloys in details, such as atoms arrangements, and site occupancy in the crystal, is fundamental in employment of these compounds in many different applications which in turn make Heusler compounds be competitor in the advanced technologies. We can describe Heusler compounds simply as they are compounds with many combinations and bonds between different elements, with particular structure, having individual properties.

A huge number of Heusler compounds have been discovered and recently guessed to be thermodynamically stable compounds with theoretical work, but they still not determined and verified experimentally.<sup>(1)</sup>

Heusler alloys are characterized by their crystal structure which is classified in the face centered cubic (fcc) structure. Fcc structure is one of the most known and observed structures in the Heusler compounds. In fcc arrangement, the atoms are located in the corners and centers of each face of faces. So the symmetry is highly findable.

They are classified into two types the first is the full-Heusler structures, the second is the half-Heusler structures, their lattice parameters value extending between  $\sim 5.6 \text{ \AA}$  to  $7.2 \text{ \AA}$ .

The lattice parameter is the length between two points on the corners of the unit cell. Constituting intermetallic compounds, with two or more metallic elements in its arrangement<sup>(2)</sup>

Heusler compounds can mainly be classified into two different sets: quaternary and ternary alloys. Quaternary Heusler compounds are chemical alloys containing four elements and have a chemical structure  $XX'YZ$  (1:1:1:1) configuration.

Ternary alloys, on the other hand, were divided into two subgroups, the first is full Heusler compounds with chemical structure  $X_2YZ$  (2:1:1) -L2<sub>1</sub>, the second one is half Heusler compounds with chemical structure  $XYZ$  (1:1:1) -C1<sub>b</sub>.

The unit cell contains four face centered cubic sublattices (fcc), each contributing to the general structure and properties of the alloy.

The unit cell occupancy varies and it's influenced by the arrangement of elements. The unit cell may be occupied by  $XXYZ$  with the positions  $(1/4, 1/4, 1/4)$  and  $(3/4, 3/4, 3/4)$  for X atom,  $(1/2, 1/2, 1/2)$  for Y atom and  $(0, 0, 0)$  for Z atoms, in this case of arrangement, the alloy forms the L21-type Full-Heusler compounds commonly known as normal Heusler structure.

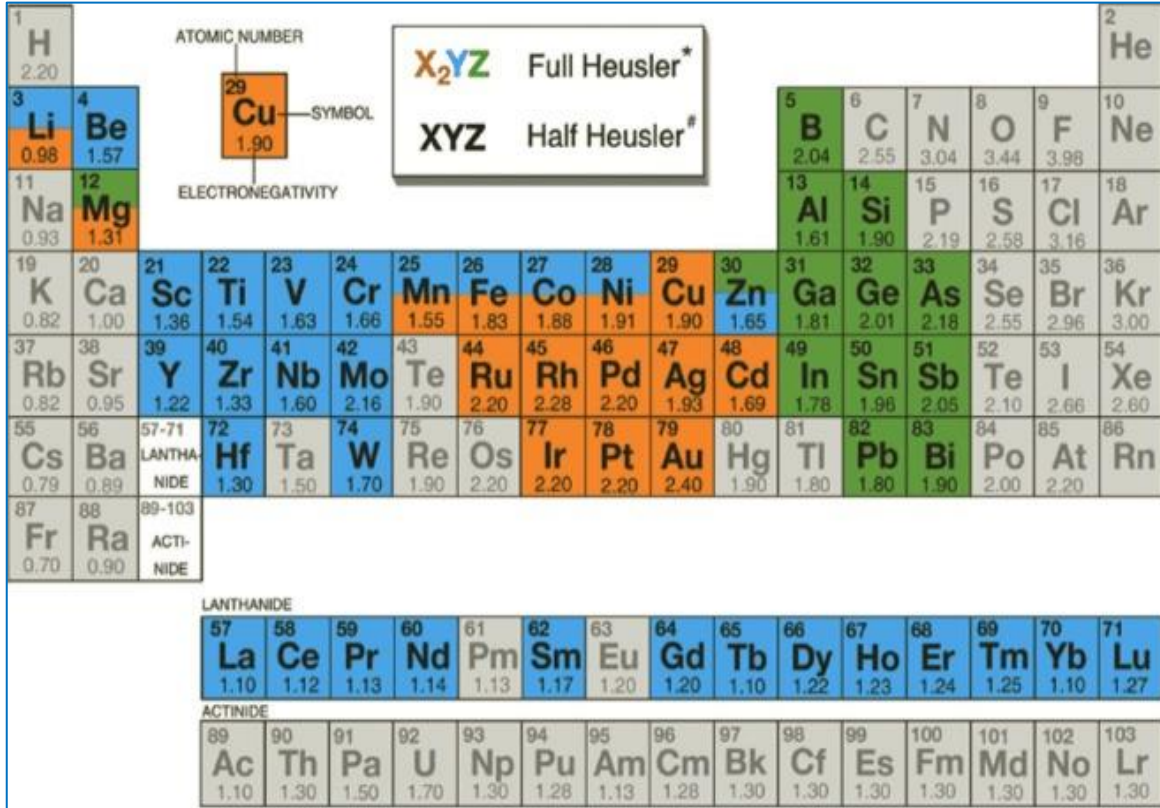
Alternatively, the unit cell may be occupied by  $XYXZ$  with the positions  $(1/4, 1/4, 1/4)$  and  $(1/2, 1/2, 1/2)$  for X atom,  $(3/4, 3/4, 3/4)$  for Y atom and  $(0, 0, 0)$  for Z atom, this configuration results the alloy forming the Xa-type Full-Heusler structure -called inverse Heusler structure. The site of the second X atom remains vacant in Half-Heusler compounds.<sup>(3)</sup>

The elements forming Heusler alloys are selected under some specific conditions as follows: X and Y denote an element from transition ones, while Z represents an element from the main group in the periodic table.<sup>(4)</sup>

The elements that can form Heusler alloys are presented in figure (1) .<sup>(5)</sup>

**Figure 1**

*Elements forming Heusler alloys  $X_2YZ$*



Within the graphical representation, the intricate arrangement between the transition elements and main group ones characterize Heusler compounds.

Transition metals are the elements located at the groups in the middle of the periodic table.

Main group elements are located at the first, second, and from thirteenth to eighteenth groups in the periodic table.

Each element's position within the crystal lattice is highlighting their roles in determining the different properties of the compound such as the properties that we focused on it in this thesis, since we examined the structural, electronic, magnetic, and elastic properties of the alloy.

### 1.3 Study Gap

In this study, the FP-LAPW method with GGA approximation has been used, serving as the cornerstone for our computational work.

mBJ is used to enhance precision and improve the calculations of the DOS and energy band gaps. Since the previous studies are not applied with this accurate approximation.

The available previous studies studied the structural, magnetic, electronic properties for these compounds.

Yilin Han et al, in 2019 have studied 171 Scandium-based full Heusler compounds by using theoretical computations to study the atomic site preferences. Their results are listed in table 1. <sup>(45)</sup>

**Table 1**

*Theoretical values from yilin Han et al study*

| Compound             |     | a(theor)<br>(Å) | MM <sub>tot</sub><br>(μB/f.u)<br>Theo. | MSc <sub>1</sub><br>(μB/f.u)<br>Theo. | MSc <sub>2</sub><br>(μB) | MM <sub>Y</sub><br>(μB) | MM <sub>Z</sub> (μB) |
|----------------------|-----|-----------------|--|---------------------------------------|--------------------------|-------------------------|----------------------|
| Sc <sub>2</sub> ZrAl | Xa  | 6.97            | 0                                      | 0.18                                  | 0.05                     | -0.08                   | -0.15                |
|                      | L21 | 7.02            | 2.47                                   | 0.5                                   | 0.5                      | 1.67                    | -0.2                 |
| Sc <sub>2</sub> ZrIn | Xa  | 7.14            | 0.77                                   | 0.14                                  | 0.33                     | 0.38                    | -0.08                |
|                      | L21 | 7.16            | 2.66                                   | 0.58                                  | 0.58                     | 1.8                     | -0.31                |

In addition, a significant departure from the previous studies of the elastic properties are investigated in this thesis for both full Heusler compounds offering a comprehensive view on the mechanical behavior for both compounds Sc<sub>2</sub>ZrAl and Sc<sub>2</sub>ZrIn.

Additionally, mBJ-GGA is very important to investigate whether the compounds are semiconductor, insulator, metal, or half metal. The half metallic study is very important for the spin polarized system.

Furthermore, the elastic properties exploration yields necessary and critical insights for studying the stability of the compounds, nature of the bonds, harmonic or inharmonic, as well as determining the materials exhibit ductile or brittle characteristics, and many other properties.

By leveraging these forward, advanced and in progress computational analysis, we aim advancing the understanding of  $\text{Sc}_2\text{ZrAl}$  and  $\text{Sc}_2\text{ZrIn}$  compounds to facilitate its various applications.

#### 1.4 Literature Review

Numerous previous studies and investigations about Heusler alloys properties of many various compounds like structural, electronic, magnetic, and elastic ones.

In 2002 Yosslen Aray et al., showed the implementation in WIEN 97 - WIEN 97 program is a perfect application of the (FP-LAPW) method, which makes more exact and careful calculations and computations of the electronic density of compounds by utilizing density functional theory and determine some important information such as the crucial points of  $\rho(r)$ , the bond paths, the graphs of the crystal, the surfaces of interatomic, and some other atomic properties.<sup>(6)</sup>

In 2004 Zhang et al., tested the transport properties of the compound  $\text{CO}_2\text{CrAl}$  and the electronic band structure. They measured the lattice parameter to be  $5.73 \text{ \AA}$ , the magnetic moment was measured to be  $3\mu_B$ , and the indirect band gap was  $0.775 \text{ eV}$ .<sup>(7)</sup>

In 2009 Ozdogan et al., resolved both the magnetic and electronic properties of  $\text{Cr}_2\text{MnSb}$  in two types, the normal and inverse structures. Their results for structural of the compound  $\text{Cr}_2\text{MnSb}$  showed that it is half-metallic.<sup>(8)</sup>

In 2010 Hakimi et al., presented a study that shows both structural and magnetic properties of full Heusler compound  $\text{CO}_2\text{CrAl}$  which was prepared by mechanical alloying. Hakimi et al. results for the calculations of the total magnetic moment was  $2 \mu_B$  for the alloy of  $\text{CO}_2\text{CrAl}$  in the normal case.<sup>(9)</sup>

In 2010 Mohammed Abu Jafar et al., calculated the structural properties for an important compound, the scandium nitride ( $\text{ScN}$ ) in the phase which called rocksalt (RS) by utilizing the (FP-LAPW) during the local density (LDA), (PBE-GGA), and other approximations. The calculations and the outcomes of their works showed that the results and the values of both the lattice parameter ( $a_0$ ), and the bulk modulus ( $B_0$ ) by using the EV-GGA and PBE-GGA approximations are more accurate than LDA and WC-GGA approximations. From their results on calculating and determining the energy

band gap of the compound by using EV-GGA+USIC platform was identified with value 1.09eV. <sup>(10)</sup>

In 2016 I. Galanakis et al. presented a survey of the electronic properties and the magnetic ones of two Heusler compounds, both the half Heusler such as: NiMnSb. And the full-Heusler such as: Co<sub>2</sub>MnGe -normal full Heusler- and Mn<sub>2</sub>CoAl -inverse full Heuslers-. With a view to talk over the origin and the source of the gap in understanding their electronic and magnetic properties they employed the first principles calculations. From their results they conclude that the total spin magnetic moment balances with the valence electrons number in the unit cell, linearly. This conclusion directly connect the magnetic to the electronic properties, so it opens the way to make and design new incoming half-metallic alloys with magnetic properties like the quaternary half-metals, magnetic semiconductors, or even the foreign spin-gapless semiconductors. <sup>(11)</sup>

In 2017, Atsufumi Hirohata et al., studied Heusler alloys in order to manage the attachments and the correlations between the magnetic properties and the crystal structures such as their conclusion “in order the antiferromagnetic Heusler alloys exhibit and show AFM behavior, it needs perfectly or partially ordered crystal structures”. <sup>(12)</sup>

In 2017 Abdelkader Boudali et al. presented quantum-mechanical calculations for the properties of the full-Heusler compounds Ti<sub>2</sub>NiX (X= Al, Ga, and In). They used the (FP-LAPW) method plus local orbital method in order to discuss the Heusler alloys based on Ti<sub>2</sub>. Results showed that the studied compounds show half metallic behavior. Over a huge domain of parameters that have been studied, the results of the calculations showed that the MM<sub>tot</sub> is 3.00 μB. The results also showed that Ti<sub>2</sub>NiX is a very promising material for spintronic applications. <sup>(13)</sup>

In 2020 Kei Hayashi et al. search on the magnetic properties of the full Heusler compounds, they conclude that the full Heusler compounds display an assortment set of magnetic status in many types like non-magnetism, ferromagnetism, ferrimagnetism and anti-ferromagnetism. They focused on the wide range of full Heusler compounds applications and how they attracted attention in many applications such as being used in the potential thermoelectric (TE) materials that turn thermal energy immediately into electricity. They also review and check the theoretical and experimental investigations on the TE properties of magnetic full-Heusler compounds. <sup>(14)</sup>

In 2020 Abu Baker et al., studied the full Heusler alloys: normal  $\text{CO}_2\text{TiSO}$  and inverse  $\text{Zr}_2\text{RhGa}$  in order to conclude the structural, magnetic, electronic, and elastic properties of these alloys by employing the FP-LAPW method. From their work results they conclude that the lattice parameter for both compounds was found to be  $6.094\text{\AA}$  and  $6.619\text{\AA}$  respectively. Also the total magnetic moment values were found to be respectively:  $1.9786\mu_B$  and  $1.99\mu_B$ . The calculations of the energy gap showed the values of the energy gap are  $0.482\text{ eV}$ . and  $0.573\text{ eV}$ ., respectively. While the elastic properties showed both of the compounds are stable. <sup>(15)</sup>

In 2021 Mohammed Abu Jafar et al., reported results for the structural, mechanical, dynamical, and electronic properties of Scandium Carbide (ScC) compound. They used the (FP-LAPW) method in accordance with (DFT), within the (GGA) approximation. Ground state properties have been computed such as the lattice constants, the bulk modulus, and the pressure derivative of the bulk modulus. The results were in good agreement with previous work. NaCl and NiAs are stable in both mechanically and dynamically phases, with NaCl considered as the ground state phase. In inequality, both compounds Zincblende (ZB) and CsCl are unstable in both mechanically and dynamically phases. <sup>(16)</sup>

In 2021 Maryam Wakeel et al. experimentally investigated the Palladium based full Heusler compounds for both the enthalpies of formations and the structural parameters. In their work they calculated many parameters such as the structural ones, the band structure, furthermore the magnetic moments. The results were accepted comparing with the available data. Their results show that all the compounds that are based on the Palladium show a metallic behavior. The ferromagnetism is strongly observed in the alloys that based on Mn, while the full Heusler alloys based on Cu, Hf, Ti and Zr are of mix magnetic state. <sup>(17)</sup>

In 2022 Qun wei et al. presented a new study with a new full Heusler compounds which are Ag-based,  $\text{Ag}_2\text{TiX}$  ( $\text{X}=\text{Ga}, \text{Ti}$ ) and  $\text{Ag}_2\text{VGa}$ . They studied the stability of the compounds, the mechanical properties, and the electronic properties for these three full Heusler compounds by utilizing the first principles calculations. Their calculations display that the compression resistance, shear resistance, stiffness, and elastic anisotropy of  $\text{Ag}_2\text{VGa}$  were higher than those of  $\text{Ag}_2\text{TiGa}$  and  $\text{Ag}_2\text{TiTi}$ , while the flexibility of  $\text{Ag}_2\text{TiGa}$  and  $\text{Ag}_2\text{TiTi}$  is improves upon that of  $\text{Ag}_2\text{VGa}$ . <sup>(18)</sup>

In a more recent study, in 2022 Al-Masri et. al., investigated the structural, electronic, magnetic, and elastic properties for both the normal and inverse Heusler  $\text{Sc}_2\text{TiAl}$  and  $\text{Sc}_2\text{TiSi}$  compounds by utilizing the FP-LAPW method. The lattice parameter was set to be for the normal  $\text{Sc}_2\text{TiAl}$   $6.8807 \text{ \AA}$ , inverse  $\text{Sc}_2\text{TiAl}$   $6.8369 \text{ \AA}$ , while for the normal  $\text{Sc}_2\text{TiSi}$   $6.6935 \text{ \AA}$  and the inverse  $\text{Sc}_2\text{TiSi}$   $6.6415 \text{ \AA}$ . The magnetic moment was found for normal  $\text{Sc}_2\text{TiAl}$   $2.72015 \mu_B$ , inverse  $\text{Sc}_2\text{TiAl}$   $2.07231 \mu_B$ , for the normal  $\text{Sc}_2\text{TiSi}$   $2.80764 \mu_B$  and the inverse  $\text{Sc}_2\text{TiSi}$   $2.20421 \mu_B$ . The electronic properties calculations show that the compounds are metallic. <sup>(19)</sup>

In 2022 Sara J. Yahya et al. investigated the full-Heusler  $\text{Co}_2\text{CrAl}$ 's structural, elastic, magnetic, and electronic properties by using the (FP-LAPW) method, which is applied in the analyzing of the structural parameters. The enhanced structural parameters were controlled by the (GGA) approximation. Through (mBJ) they estimated the energy gaps for the alloys, and it was accomplished. From their results it was concluded that the normal Heusler compound with mBJ and GGA approximations show a half-metallic phase, and there is an energy gap in the spin-down configuration. The total magnetic moments for the two compounds were agreeable with the theoretical and experimental calculations previously achieved. Mechanically, they found that the normal and inverse full-Heusler compound  $\text{Co}_2\text{CrAl}$  was stable. <sup>(20)</sup>

In 2022 Yazeed Alnafie et al. studied some properties such as the structural properties, and the electronic properties of simultaneously full and half Heusler compounds  $\text{Fe}_2\text{NbIn}$ ,  $\text{FeNbIn}$  respectively by utilizing the density functional theory evaluations. The calculations have been executed utilizing (GGA) method. Their results showed that Heusler compounds are stable and metallic structure. While the results that related to the band gap, they investigated that  $\text{Fe}_2\text{NbIn}$  has a small band gap. <sup>(21)</sup>

In 2022 Cheifa Harimek et al. presented a study that discuss the ferromagnetism and many additional properties in some Heusler Co-based compounds, the full Heusler compound  $\text{Co}_2\text{CrAl}$  and the half Heusler compound  $\text{CoCrSb}$ . They investigated the Full and Half Heusler compounds theoretically, based on the (DFT). They also investigated several properties like: structural, electronic, magnetic, and elastic with the utilizing of the first principles calculations. As a result of their calculations, and since the two energies values are negative, cohesive and formation, the compounds show a half metallicity and their total magnetic moment is an integer number. These results are in

dealing with the Slater Pauling rule. Also they obtain that the compounds are stable mechanically from the elastic properties' calculation.<sup>(22)</sup>

In 2023 Zainab Mualla et al. studied the structural, electronic, and mechanical properties of (RbI) rubidium iodide. Their results have been inspected by employing the (GGA) approximation and the (FP-LAPW) method. Utilizing the (mBJ) approximation the potential was roughly calculated, which expanded the regulation of the electronic properties. In their work, they analyzed RbI in a broad expanse of crystal structures, including topologies like rock salt (RS), CsCl, zinc blende (ZB), NiAs, and wurtzite (WZ), among others. Their investigation display a powerful connection between the material's physical properties and the results and data concluded and drawn from both theoretical and experimental research.<sup>(23)</sup>

In 2023 Raed Jaradat et al. studied the electronic, magnetic, and optical properties of NaS and NaSe compounds with the first principle calculations. The (PBE-GGA) and the (mBJ-GGA) have been utilized to transact with the exchange-correlation potential. The PBE-GGA and mBJ-GGA electronic calculations display an enclosing behavior in the spin-up configuration, a metallic behavior shown in the spin-down configurations. In extension, both PBE-GGA and mBJ-GGA correspond that the total magnetic moment per unit cell for these compounds is 1  $\mu\text{B}$ .<sup>(24)</sup>

In 2023 Nazmiye Kervan et al. calculated and analyzed the structural, electronic, magnetic, and optical properties of the full Heusler alloy  $\text{Ti}_2\text{RuAl}$  by utilizing the first principles calculations that established on the (DFT) and the (GGA) approximation in the Wien2k package. From their results,  $\text{Ti}_2\text{RuAl}$  full Heusler compound presents a ferrimagnetic half metallic behavior. And the calculations of the total magnetic moment was 1  $\mu\text{B}$ . This value was in dealing with the Slater Pauling rule.<sup>(25)</sup>

In 2023 P. Singh et al. used two computational methods to make consideration of Full heusler compounds. First is the pseudo-potential method used in the Atomistic Tool Kit-Virtual Nanolab, while the second is FP-LAPW method which executed in WIEN2k. Computationally, these compounds show metallic behavior. According to the WIEN2k, the magnetic moments of the compounds  $\text{Co}_2\text{CrZ}$  ( $Z = \text{As, B, Ga, and Pb}$ ) are 4.93  $\mu\text{B}$  and 5.02  $\mu\text{B}$ , 3.00  $\mu\text{B}$  and 3.08  $\mu\text{B}$ , 3.02  $\mu\text{B}$  and 3.16  $\mu\text{B}$ , and 4.07  $\mu\text{B}$  and 4.30  $\mu\text{B}$ , respectively. The results of the elastic properties,  $\text{Co}_2\text{CrZ}$  compounds are ductile with Z

= As, Pb, while the compounds with Z = B, Ga are brittle.  $\text{Co}_2\text{CrZ}$  (Z = As, B, Ga, and Pb) compounds show metallic behavior since  $(\text{CP} = \text{C12} - \text{C44})$  value is positive.<sup>(26)</sup>

In 2023 Ismail Ait Elkoua et al. studied the structural, electronic, magnetic, optical, and thermoelectric properties of the inverse full Heusler compounds  $\text{Ag}_2\text{TiGa}$  and  $\text{Ag}_2\text{VGa}$ . They used the density functional theory based on the wien2k software, in addition to the computational methods: GGA, GGA-mBJ, and other computational methods. The band structures (BS) of the compounds show that they are both metallic.

In 2023 Jabar Abderrahim et al. presented a study that discuss the physical properties such as: structural, magnetic, electronic, optical, and thermoelectric characteristics of the Full-Heusler compound  $\text{FeCuMnSi}$  by using the (DFT) that executed in the Wien2k software. The exchange correlation potential has been performed in combination with the GGA-PBE and the (mBJ). They found that the compound they studied exhibit a half-metal character.<sup>(27)</sup>

In 2023 Quratul Ain et al. studied the electronic structure, elastic, optical and transport characteristics of full Heusler  $\text{Na}_2\text{TlX}$  (X=Bi, Sb) alloys using the (DFT). For the purpose of analyzing the electronic properties they utilize the (mBJ). Both of the compounds are in stable phases because of the negative formation energies. Moreover, both of the compounds are exhibiting semiconductor nature.<sup>(28)</sup>

In 2023 Jyoti Kapil et al. studied the structural, electronic, magnetic, and elastic properties of Full-Heusler compound  $\text{Ru}_2\text{VSi}$  by using density functional theory (DFT). They performed the calculations by using the (GGA). And the results show that the compound in both the spin up and down states presents a metallic behavior, and the magnetic moment is with non-integral, this result is in deal with the Slater-Pauling Rule. The studied properties let this compound an appropriate material for the spintronic devices applications.<sup>(29)</sup>

In 2023 Abbas Charef et al. used the (FP-LAPW) method, which based on (DFT) in addition to the (GGA) approximation and the (mBJ), to consider the structural, elastic, electronic, and optical properties of the full Heusler compounds  $\text{Na}_2\text{SrX}$  (X= Si and Ge). From their results, they conclude that the compounds show a nonmagnetic

structure. As for the calculations of the electronic BS and the DOS they conclude that the compounds show semiconductor attitude.<sup>(30)</sup>

In 2024 Ismail Ait Elkoua et al., investigated the structural, electronic, magnetic, and mechanical properties of the full Heusler compounds TiHFeX ([X: Ga, In). They used some approximations implemented in the DFT and integrated in the WIEN2K software such as: GGA-PBE, TB-mBj, GGA-PBEsol, and GGA-WC. Their results show that the full Heusler compounds they have examined are assumed in the ferromagnetic phase with various structural stabilities. As for the band structure calculations and total electron (DOS) investigates that these compounds are semi-metals. The elastic constants emphasize its steadiness presented by various elastic constants like the Cauchy pressure, Poisson's ratio, the anisotropy factor, Young's modulus, and the shear modulus.<sup>(31)</sup>

### **1.5 Importance of this thesis**

After reviewing previous studies and scientific research on Heusler compounds, the selection of the compounds to which we devoted this study was not in vain, but rather was due to the lack of previous studies on them.

New results are presented in this thesis that concern the metallicity of  $\text{Sc}_2\text{ZrAl}$  and  $\text{Sc}_2\text{ZrIn}$  compounds, along with an investigation into different other properties by utilizing FP-LAPW procedure based on DFT.

The following key determinations have been made:

- **The structural properties:** Fundamental characteristics of the crystal structure like lattice parameters, first pressure derivatives and bulk modulus.
- **The electronic properties:** exploration of band structure, energy gap and density of state (DOS) display shrewdness into the electronic behavior of the compound.
- **The magnetic properties:** Estimating the magnetic moments provides critical and useful information on the compound magnetic behavior.
- **The elastic properties:** Assessment of the elastic constant, bulk modulus, shear modulus, Poisson's ratio ( $\nu$ ), and anisotropic factor (A) explain the material's

mechanical response for different conditions and understanding its mechanical stability.

These properties have been analyzed and investigated by using the WIEN2k software on the full Heusler compounds  $\text{Sc}_2\text{ZrAl}$ ,  $\text{Sc}_2\text{ZrIn}$  and compared with ones available in previous results to enhance the understanding of these compounds behavior.

After one study these properties, he will get important results and information that let him capable to know the nature of the compound and use it in previous and useful applications depending on these properties.

One can determine if the compound is semiconductor, insulator, metal, or half metal and in turn substantial for the polarizing system. We can also know if the compound is stable or not, ductile or brittle.

The finding results are presented in this thesis, laying the groundwork for further research. Our study focuses on characterizing the structural, magnetic, electronic, and elastic properties of the Full-Heusler compounds:  $\text{Sc}_2\text{ZrAl}$  and  $\text{Sc}_2\text{ZrIn}$  using the full potential linearized augmented plane wave FP-LAPW method. Since we used the mBJ approximation we have improved the calculations and tabulated it in this thesis.

The methodology employed in this investigation is presented in chapter two. The computational method we used, WIEN2K software, is explained in chapter three. In chapter four the results and discussion derived from our analysis are shown. Finally, in chapter five the conclusion is summarized.

## Chapter Two

### Methodology

To determine the quantitative properties of solids, that we aim to obtain –structural, electronic, elastic, and magnetic properties of the full Heusler compounds we need to think through with a view to solve the time independent Schrödinger Equation (SE) for N-body system.

$$\hat{H}\Psi = E\Psi \quad (1)$$

Where H represents the Hamiltonian of N-body system,

E represents the energy of N-body system,

$\Psi$  represents the wave function of the involved particles in the system.

Equation (1) represents the system's total energy, the eigenvalues, and the system's eigenstates. In addition to the information about the system's stationary states.

By solving this equation, we can realize the molecules and solids quantum behavior.

The Hamiltonian is defined as,

$$\begin{aligned} \hat{H} = & -\frac{\hbar^2}{2} \sum_{i=1}^N \frac{\nabla_{\vec{R}_i}^2}{M_i} - \frac{\hbar^2}{2} \sum_{i=1}^N \frac{\nabla_{\vec{r}_i}^2}{m_e} - \frac{1}{4\pi\epsilon_0} \sum_{ij} \frac{e^2 Z_i}{|\vec{R}_i - \vec{r}_j|} + \frac{1}{8\pi\epsilon_0} \sum_{i \neq j} \frac{e^2}{|\vec{r}_i - \vec{r}_j|} \\ & + \frac{1}{8\pi\epsilon_0} \sum_{i \neq j} \frac{e^2 Z_i Z_j}{|\vec{R}_i - \vec{R}_j|} \end{aligned} \quad (2)$$

Where  $\hbar = \frac{h}{2\pi}$ , h is Plank constant =  $6.626 \times 10^{-34}$

$\nabla^2$  is the Laplacian =  $\frac{\partial^2}{\partial x^2} + \frac{\partial^2}{\partial y^2} + \frac{\partial^2}{\partial z^2}$ ,

M is the mass of the nuclei,

$m_e$  is the mass of the electron,

$\epsilon_0$  is the vacuum permittivity =  $8.85 \times 10^{-12} \frac{C^2}{N.m^2}$

$e$  is the electron charge =  $1.6 \times 10^{-19} \text{ C}$

$Z$  is the atomic number,

$R$  is the atomic radius,

$r$  is the nuclei radius.

The first term in this equation represents the kinetic energy operator for the nuclei ( $T_n$ ), the second term is for the electrons' kinetic energy ( $T_e$ ).

The final three terms characterize the coulomb interaction between electron and nuclei ( $V_{en}$ ), electron and other electrons ( $V_{ee}$ ), nuclei and other nuclei ( $V_{nn}$ ) respectively.

This SE can't be solved exactly for many-body system. So here are several approximations help to clarify the problem:

### **2.1 The Born-Oppenheimer Approximation (BOA)**

The Born-Oppenheimer approximation (BOA) is an essential approximation in quantum science, almost fixedly the obligatory starting point for the quantum-mechanical treatment of the molecular systems.

(BOA) states that we can deal with the nuclei and the electrons separately because of their masses difference. So we can make a configuration that nucleus is fixed.

It is based on the separation of the electronic and nuclear degrees of freedom, which is possible because of the huge difference between these two particles masses.<sup>(32)</sup>

Since the nucleus is very massive and weighty compared to the electron - about 1000 times more - it is slower than the electron, therefore this approximation assumes that the nuclei are fixed in position.

So according to BOA  $T_n$  can be dropped and  $V_{nn}$  will be reduced to a constant.

Therefore, equation (2) can be written as:

$$\hat{H} = \hat{T}_e + \hat{V}_{en} + \hat{V}_{ee} + \hat{V}_{nn} \quad (3)$$

$$\hat{H} = \hat{T}_e + \hat{V}_{ee} + \hat{V}_{ext} \quad (4)$$

Where  $V_{ext} = V_{en} + V_{nn}$  and called the external potential.

The many-particle problem become simpler, but it is still difficult to be calculated, and the complexity represented in  $V_{ee}$  term. <sup>(33)</sup>

## 2.2 Hartree and Hartree-Fock Approximation

Hartree and Hartree-Fock approximations are used to solve (SE) within (BOA) framework.

In Hartree approximation, the interaction between electrons "electron-electron" interactions is considered mean field come from the other electrons, and their correlations are neglected.

This approximation is logical and sensible one for the true electron system, but it fails for electron-electron correlation.

The approximation assumption:

This approximation is based on simulating that the electrons are free and independent of each other.

Hartree-Fock approximation is a variational technique. It can be exercised at both temperatures zero and finite ones, at equilibrium and out of equilibrium, the so-called time-dependent Hartree-Fock approximation that returns linear reaction functions appropriate and suitable with conservation laws. <sup>(34)</sup>

The Hartree-Fock approximation upgrade the Hartree one by inserting an antisymmetrization requirement for the wave function due to the fermionic nature of electrons.

It minimizes the energy according to the variation in orbitals, so this approximation includes some electrons correlations. By doing this Hartree-Fock approximation is more accurate than Hartree approximation.

Both the Hartree and Hartree-Fock approximations are methods are basic for electron correlation effects more with more accurate calculations.

So the system of N electrons can be described by the wave function ( $\psi$ ), which can be set up as:

$$\psi_n(r_1, r_2, r_3, \dots, r_N) = \psi_1(r_1)\psi_2(r_2)\psi_3(r_3)\dots\psi_N(r_N) \quad (5)$$

Besides, the overall Hamiltonian can be set up as:

$$\hat{H} = \hat{T}_e + \hat{V}_{\text{ext}} + \hat{V}_H \quad (6)$$

Where  $T_S$  express the kinetic energy,

the external potential is described by  $V_{\text{ext}}$ ,

and  $V_H$  is the Hartree potential which is defined as:

$$\hat{V}_H = \frac{1}{8\pi\epsilon_0} \sum_{ij}^N \frac{|\psi(\vec{r}_i)|^2 |\psi(\vec{r}_j)|^2 d^3r_i d^3r_j}{|\vec{r}_i - \vec{r}_j|}. \quad (7)$$

This method has a huge computational effort, which makes it an additional and extra complex system, and this is the enormous issue.<sup>(35)</sup>

### 2.3 Density Functional Theory (DFT)

(DFT) nominates as a fundamental technique in computational quantum chemistry and materials science because of its cleverness and scalability. It is a strong approximation in studying the electronic structure of solids. Which in turn supplies a framework to guess the electronic behavior in solids.<sup>(35)</sup>

This approximation was founded by Hohenberg and Kohn in 1964, it considers the electron density as the fundamental measure as an alternative of the wave function of many electrons.

By DFT the many-body problem can be solved as a one-body problem (non-interacting system with the selfsame whole density). Since it deals with the electron density to be the major quantity of attention.

When research apply DFT on (SE) this make them able to study distinct properties of alloys with a wonderful and noteworthy accuracy.

It is efficient to minimize the effective energy which will command to the ground state density ( $\rho_0$ ).

Thus  $E(\rho)$  can be set up again as the Hartree overall energy in addition to smaller anonymous functional term called exchanged-correlation functional  $E_{xc}(\rho)$ .

$$E(\rho) = T_s(\rho) + E_c(\rho) + E_H(\rho) + E_{ii}(\rho) + E_{xc}(\rho) \quad (8)$$

where  $T_s$  refers to single kinetic energy,

$E_c$  is coulomb energy between nuclei and electrons,

$E_{ii}(\rho)$  the interaction between nuclei,

$E_{xc}$  is exchange correlation energy, which is an unknown part

and  $E_H$  is Hartree potential which is defined as:

$$E_H(\rho) = \frac{e^2}{2} \int d^3r d^3r' \frac{\rho(\vec{r})\rho(\vec{r}')}{|\vec{r} - \vec{r}'|} \quad (9)$$

Schrodinger Equation (SE) for a one electron problem can be written as:

$$[T_s + V_{\text{ext}}(r) + V_H(\rho(r)) + V_{xc}(\rho(r))] \Phi_i(r) = \varepsilon_i \Phi_i(r) \quad (10)$$

Where,  $\varepsilon_i$  is the single particle energy,

$\Phi_i$  is the electron wave function,

$V_H$  is the Hartree potential,

$V_{ext}$  the coulomb potential,

and  $V_{XC}$  is the exchange-correlation potential. <sup>(36)</sup>

## 2.4 Single particle Kohn-Sham Equation

(DFT) does not supply any beneficial and useful computational platform. The path to convert it into usable is founded on the Kohn and Sham though to project the interacting electron gas into a non-interacting reference or helpful system.

Single particle Kohn-Sham equation is an important key in (DFT), it's a computational method founded in 1965, by Walter Kohn and Lu Jeu Sham. This method can be considered as a means for solving the electronic structure system, it's derived from Hohenberg theorems, and these theorems steady the survival and existence of an energy function of the electron density.

This method chart the system as a non-interacting electrons system in motion with an effective potential. This effective potential depends mainly on the electron density. Kohn Sham method can be considered as an efficient method for studying the electronic properties of solids.

Further detailing, the Kohn-Sham ansatz exchange the issue of interacting electrons by a helpful free-particle issue, where whole many-body impact behind the Hartree term are inclusive in a clear exchange-correlation functional. <sup>(37)</sup>

By using LAPW method, Kohn-Sham (KS) equation of a many-electron system for the density of the ground state, in addition to the total energy, and KS eigenvalues (energy bands) were solved.

This expression can be expressed as the effective energy of a non-interacting classical electron gas, liable to two external potentials: the first potential is due to the nuclei  $\hat{V}_{ext}[\rho]$ , and the second one is because of the exchange and correlation effects  $\hat{V}_{xc}[\rho]$ .

The exact ground-state density  $\rho(r)$  of an N-electron system is given by:

$$\rho(\vec{r}) = \sum_{i=1}^N \phi_i^*(\vec{r})\phi_i(\vec{r}) = \sum_{i=1}^N |\phi_i(\vec{r})|^2, \quad (11)$$

Where  $\phi_i(\vec{r})$  is the single-particle wave functions, which are the N lowest-energy solutions of the KS equation.

$$\hat{H}_{KS}\phi_i = \epsilon_i\phi_i \quad (12)$$

KS equation sometimes is written as:

$$\hat{H}\phi_i(\vec{r}) = \left[ -\frac{\hbar^2}{2m_e}\vec{\nabla}_i^2 + V_{eff} \right] \phi_i = \epsilon_i\phi_i \quad (13)$$

Where  $\hat{H}$  is the Hamiltonian operator.

The effective potential  $V_{eff}(\vec{r})$  is the sum of the external, the Hartree (electrostatic), and the exchange-correlation potentials:

$$V_{eff}(\vec{r}) = V_{ext}(\vec{r}) + \frac{\delta E_H[\rho]}{\delta \rho} + \frac{\delta E_{xc}[\rho]}{\delta \rho} = V_{ext}(\vec{r}) + \frac{e^2}{4\pi\epsilon_0} \int \frac{\rho(\vec{r}')}{|\vec{r} - \vec{r}'|} d\vec{r}' + V_{xc}(\vec{r}) \quad (14)$$

From this equation,  $V_H$  and  $V_{xc}$  count on the charge density  $\rho(\vec{r})$ , which also count on  $\phi_i$  which is being seek.

That means we are transiting with a self-consistency problem. The solution  $\phi_i$  define the operators  $V_H$  and  $V_{xc}$  in  $H_{KS}$  in the main equation.

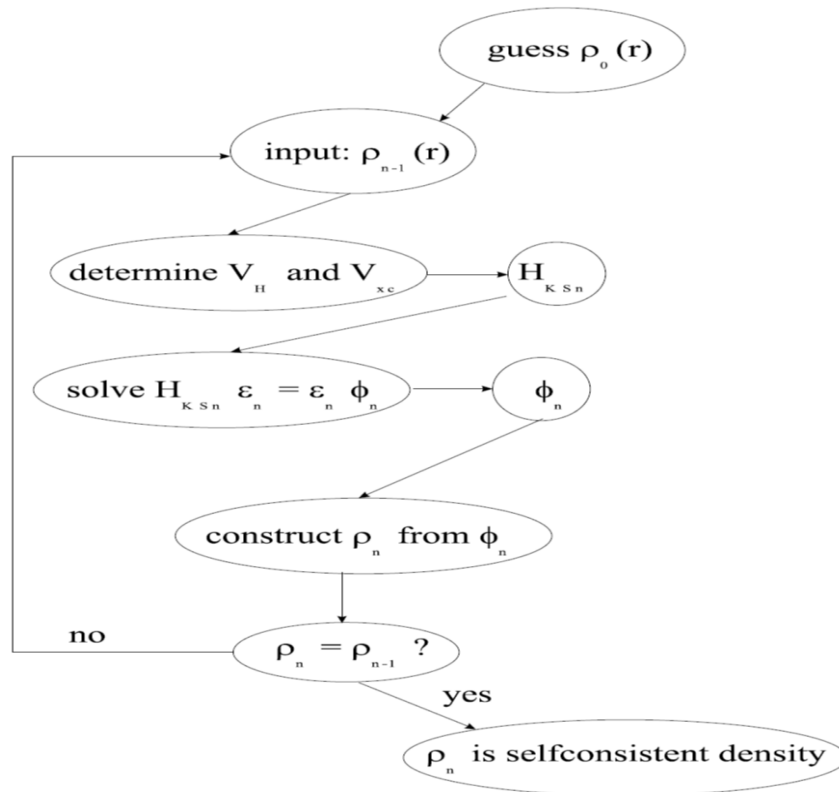
We can't write down this equation and fix it unless we determine its solutions. Some beginning density  $\rho_0$  is estimated, and a Hamiltonian  $H_{KS1}$  can be originated from it. The eigenvalue problem is solved, and  $\phi_1$  can be specified from  $\rho_1$ .

Now  $\rho_1$  can be applied to tribute and make construction for  $H_{KS2}$  that will give  $\rho_2$  as an output, etc. The steps can be used until the chain converge and  $\rho_f$  become an output. <sup>(38)</sup>

These steps are presented in figure (2).

**Figure 2**

*The scheme for the  $n^{th}$  relationship in the self-consistent steps to clarify Hartree-Fock or Kohn-Sham equations*



## 2.5 The Exchange-Correlation Functional

Since no one else rough calculations were made excluding the previous Born-Oppenheimer approximation, we can consider that the approximation KS scheme is very accurate. But we still don't know the functional exchange-correlation yet, so we need to introduce more approximations.

The Exchange-Correlation Functional is a decisive method in (DFT), it's utilized in describing the interactions between the electrons in the N-electron system.

This method converges the exchange correlation energy, which emerge from Pauli Exclusion Principle.

Pauli Exclusion Principle was founded in 1925, by Wolfgang Pauli, which states that "it's impossible for any two electrons in the atom to have the same four quantum number".

The exchange term in the system considerations for the antisymmetric of the wavefunction is answerable about the exchange interaction. It characterizes electron-electron interactions involving the repulsion between them.

Several shapes of the Exchange correlation function, different with their accuracy. Two of the most famous examples of approximations used toward this goal are: The Local Density Approximation (LDA) and The Generalized Gradient Approximation (GGA).<sup>(36)</sup>

## 2.6 Local Density Approximation (LDA)

LDA was applied to DFT by Kohn and Sham. The functional exchange-correlation can be approximated as a local function since it's not known exactly. Show up to a fresher qualitative process to the consideration of the electronic systems, beginning with the atoms, molecules, condensed matter systems – studying substances in their solid state- and macromolecules – huge molecule, commonly with a diameter extending from about 100 to 10,000 angstroms- particularly and other fermionic systems broadly.<sup>(39)</sup>

LDA supposes the exchange correlation energy to be influenced by the local electron density at some offered points. So (LDA) can supply accurate results for different systems, essentially for the systems that have slow diverging in the density of electron.

LDA can be solved by the exchange-correlation energy, it would be given as:

$$E_{xc}^{LDA} = \int \rho(\vec{r}) \epsilon_{xc}[\rho(\vec{r})] d\vec{r} \quad (15)$$

Where the  $\epsilon_{xc}[\rho(\vec{r})]$  is the exchange-correlation energy per electron of a homogenous electron gas, whose electronic density is precisely  $\rho_0(r)$  at any  $r$ .

The LDA approximation will be useful whenever the electronic density modify bit by bit with the position due to lack of  $\rho_0(r)$  derivative in the phrase for  $\epsilon_{xc}[\rho(\vec{r})]$ , which indicates by the term "local".

If the exchange and correlation assistances are counted individually one by one, the first contribution will be calculated analytically.

The Correlation energy is elected by as a complicated function of  $\rho_0$  consisting on the parameters whose values are suitable by employing an accurate and careful simulation of the homogeneous electron gas energy as a reference point.

$$E_{xc}^{LDA} = E_x^{LDA} + E_c^{LDA} \quad (16)$$

The primary phrase is the exchange energy which occurs from the Pauli Exclusion Principle, meanwhile the second term, known as the correlation energy which occurs from the interaction of electrons with the identical spin. <sup>(35)</sup>

## 2.7 Generalized Gradient Approximation (GGA)

The generalized gradient approximation (GGA) is an expansion and a spread of (LDA), this approximation takes besides the electron density, its gradient in account. So there's further phrases determined by on the electron density's gradient, these terms granting more accurate characterization and improving the precision of LDA.

(GGA) depends indirectly on the Kohn-Sham (KS) orbitals through the kinetic energy density i.e., not given by an obvious term. <sup>(40)</sup>

This approximation improves the clarification of the local spin density (LSD) of the exchange-correlation energy by counting the first derivative of the electron density.

While LDA employs the exchange energy density of the regular electron gas, ignoring the homogeneity of the real charge density, GGA be alert of such inhomogeneity by making inclusion for the gradient of the electron density  $\vec{\nabla}\rho(\vec{r})$  in the function.

$$E_{xc}^{GGA} = \int \rho(\vec{r}) \epsilon_{xc}[\rho(\vec{r}), \vec{\nabla}\rho(\vec{r})] d\vec{r} \quad (17)$$

Where  $\rho(\vec{r})$  is the charge density, and  $\vec{\nabla}\rho(\vec{r})$  is the gradient of charge density.

GGA was found to be more accurate than the LDA in electronic structure calculation. <sup>(35)</sup>

Both of LDA and GGA approximations are very usable in DFT, to choose one of them, this depends on the system under study, in addition to the calculation's accuracy required.

## 2.8 Augmented Plane Wave (APW) Method

To study the materials' electronic structure APW and its techniques are used computationally. APW extends the wave function with additional terms that related to plane waves in the crystal. Other terms near to the atomic locations, these terms are called augmentation function.

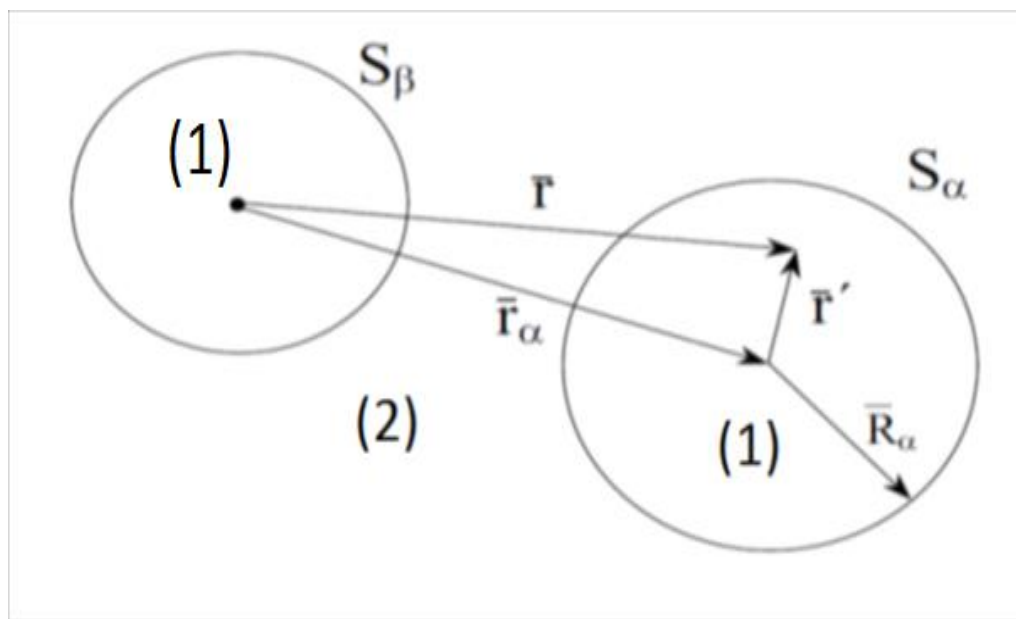
These augmentation functions secure that the wave function satisfy the boundary conditions near the atomic sites, which leads to more accurate calculations in this region.

In APW method, the unit cell is split to two zones. The first one is separated atomic spheres concentrated at the atomic positions; like a sphere is called a muffin tin ( $S_\alpha$ ) with radius  $R_\alpha$ .

The second is the surviving space outside the spheres which is called the interstitial zone or the interstitial region, as demonstrated in figure (3).

**Figure 3**

*Scheme of Augmented Plane Wave*



If the electrons are far from the nuclei, they are considered almost free, and therefore we can describe them as plane waves. But if they are adjacent to the nuclei, they manage as if it were in a free atom, so we have the ability to use atomic like functions.

APW applied make expansion of  $\phi_n$  clarified as:

$$\phi_{\vec{k}}(\vec{r}, E) = \begin{cases} \frac{1}{\sqrt{V}} e^{i(\vec{k}+\vec{K})\cdot\vec{r}} & , \quad r > R_\alpha \\ \sum_{l,m} A_{lm}^{\alpha,\vec{k}+\vec{K}} u_l^\alpha(\vec{r}', E) Y_l^m(\vec{r}') & , \quad r' < R_\alpha \end{cases} \quad (18)$$

where  $\vec{k}$  is the wave vector inside the Brillion zone,

$\vec{K}$  is the reciprocal lattice vectors,

V is the volume of the unit cell,

$r'$  is the position vector inside the sphere,

and  $u_l^\alpha$  is the radial part solution of SE at energy  $\varepsilon$ .<sup>(36)</sup>

## 2.9 The Linearized Augmented Plane Wave (LAPW) Method

LAPW make a linearization of the function concerning the atomic sites, so it can be considered to be a more functional computational approximation.

LAPW method expands the wave function in terms of spherical harmonics and radial functions, so the solution will be simplified.

This approximation procedure is a method for resolving the KS equation. This scheme, which looks like APW was introduced by Anderson. He suggested expanding the energy reliance of radial wave functions  $u(r')$  inside the atomic spheres with its energy derivative  $\frac{\partial u^\alpha(r', E)}{\partial E} = \dot{u}^\alpha(r', E)$ .

A linear series of radial function times spherical harmonics is applied in this scheme.

For a sphere of radius  $R_\alpha$ , spherical harmonic  $Y_{lm}(r)$  is utilized where  $u_l(r, E_l)$  is the normal solution of the radial SE for energy  $E_l$ , and the spherical part of the potential inside sphere  $\dot{u}^\alpha(r', E)$  is the energy derivative of  $u_l$  taken at the same energy.<sup>(36)</sup>

$$\phi_{\vec{k}}^{\bar{k}}(\vec{r}, E) = \sum_{l,m} ( a_{lm}^{\alpha, \vec{k}+\vec{K}} u_l^\alpha(\vec{r}', E) + b_{lm}^{\alpha, \vec{k}+\vec{K}} \dot{u}_l^\alpha(\vec{r}', E) ) Y_m^l(\vec{r}') \quad , r' < R_\alpha \quad (19)$$

In the interstitial region this expansion for plane wave is utilized:

$$\phi_{\vec{k}}^{\bar{k}}(\vec{r}, E) = \frac{1}{\sqrt{V}} e^{i(\vec{k}+\vec{K})\cdot\vec{r}} \quad , \quad r > R_\alpha \quad (20)$$

In common form LAPW method extends and develops the potential as the subsequent frame:

$$V(\vec{r}) = \begin{cases} \sum_{lm} V_{lm}(r) Y_{lm}(\vec{r}) & \text{inside sphere} \\ \sum_{\vec{k}} V_{\vec{k}} e^{i\vec{k}\cdot\vec{r}} & \text{outside sphere} \end{cases} \quad (21)$$

## 2.10 Modified Becke-Johnson Potential (mBJ)

mBJ was founded and designed to develop the worthiness of DFT calculations. Especially for the calculations of the band gabs of the semiconductors and insulators materials.

mBJ contains some parameters related to make fitting with the data collected from the experimental works. This approximation is utilized to enhance the band structure of materials, particularly semiconductor materials to be comparable with the experimental results. It is a system that is highly substantiated and is utilized in the WIEN2k code.

As a result, it is significant in terms of general agreement with the experiment. As a consequence of the absence of an exchange and correlation energy term from which to deduce the mBJ potential, a straight optimization to determine the lattice parameter is not feasible.

The experimental gap value can diverge by as much as 20-40 percent. It was offer and suggested that the LDA, GGA optimization approach was once upon a time used to compute the band structure and the output network parameter, and this offer is decisive considering that the percentage variations in the lattice parameter can generate relative deviations in the expected band gap. <sup>(41)</sup>

mBJ is commonly used with other techniques such as LAPW approximation to improve the calculations of determining some properties such as band structure of the electron.

## Chapter Three

### Results

#### 3.1 General look on WIEN2k

In our work, we used the WIEN2k computer program, WIE2k is a software package, a very powerful computational method which is documented in FORTRAN language, runs under Linux system. Available in English language. It is universally applied in solid state physics and material science.

The original authors of WIEN2k are P. Blaha, K. Schwarz, F. Tran, D. Kvasnicka, and R. Laskowski. WIEN2k developed by the Institute of materials chemistry, TU Wien. It is used widely in quantum calculations. <sup>(13)</sup>

The term WIEN2k derives from two sections, the first "WIEN" and the second "2k", WIEN derives from the name of the computational code improved by Peter Blaha et. al., since they improved this code at Vienna University, they called the code "WIEN" related to the university name. While the second term "2k" refers to the code's generation which was the second generation. <sup>(17)</sup>

The first code was done by using WIEN2k in 1990. After that, there are many releases WIEN93, WIEN97 and the last one is WIEN2k with many versions the newest one is WIEN2k-23.2 which was done in February 2023. More than 3400 user groups has licensed the WIEN2k. WIEN2k calculates the electronic structure by utilizing the DFT.

To install WIEN2k, you need a memory with at least 1GB, with Linux in your PC. It is an open-source package, available free for scientific community.

WIE2k package is used in order to study the electronic structure, WIEN2k based on DFT, employing (FP-LAPW) method, to answer Kohn-Sham equations, which in sequence help to make accurate investigations for the properties of the solids. So researchers are able to understand the solid-state physics and material science.

Many advantages encourage us to use WIEN2k software, since WIEN2k utilize FP-LAPW method, so it becomes common with its precision and accuracy. Also WIEN2k is very versatile, which means capable of classifying the materials from metals, semiconductors, to complex alloys.

WIEN2k is very flexible, which make it very useful to study many properties of the compound and calculate many parameters. Because of that, scientists and researchers are able to study many applications as the magnetisity, superconductors, and topological insulators.

As we have mentioned before WIEN2k is available free, which is a very good advantage, in addition to this, the users of WIEN2k are very friendly, this is what happened with us during our works, as we communicated with some of them and got answers to some technical issues, WIE2k also provides tutorials in order to help researchers. Which facilitate the calculations, analyzing data, and the outcomes.

WIE2k merges progress tools that qualify the researchers exploring the results effectively, such as plot electronic band structures and DOS, so one can imagine the magnetic properties of the compound.

### **3.2 WIE2k techniques**

WIEN2k utilizes different approximations to study the solids and their electronic structure. It's based basically on DFT, which is a computational quantum mechanical modelling method being implemented in the WIEN2k software package. It's an efficient method to determine the electronic structure. <sup>(13)</sup>

In this study, structural, electronic, elastic, and magnetic properties of the Full-Heusler Compounds:  $\text{Sc}_2\text{ZrAl}$ ,  $\text{Sc}_2\text{ZrIn}$  are inspected using -FP-LAPW- method.<sup>(42)</sup> This process supplies more exact and accurate determinations of the electronic structure of atoms. FP-LAPW method split the unit cell to two regions, this expands the wave function and make a good accuracy.

FP-LAPW- method is an application of Kohn-Sham density functional theory (DFT), which typically goes with the study of core and valence electrons, the ground state density, total energy, and Kohn-Sham eigenvalues (energy bands) of a many-electron system. <sup>(13), (17)</sup>

In our work, we employed the (GGA) in order to rank the structural parameters (bulk modulus, lattice parameters and first pressure derivatives)

Also, the (mBJ) is used computationally to progress the calculated value with better results of energy band gap for these compounds. This approximation was a wonderful feature in our work, as the previous work didn't employ it.

Augmented plane wave method (APW) uses muffin-tin approximation. It expands the wave function with terms related to plane waves close to the atomic nuclei to converge the energy states of an electron in a crystal lattice.

The muffin-tin approximation was proposed by Joh C. Slater, a shape approach of the potential well in the crystal lattice. Most ordinary used in quantum mechanical simulations of the electronic band structure in solids. Muffin-tin radii ( $R_{MT}$ ) for the compound  $Sc_2ZrAl$  are: 2.5, 2.5 and 2.5 a.u for Sc , Zr and Al ,respectively. For the compound  $Sc_2ZrIn$ ,  $R_{MT}$  are 2.5, 2.5 and 2.5 a.u for Sc, Zr and In, respectively.

To obtain a self-consistency for the compounds, 165 particular K-points in the irreducible Brillion Zone (IBZ) were applied with a connection to 5000 K-points in the full BZ.<sup>(42)</sup>

Also the plane wave number was bounded by:

$$K_{max} R_{MT} = 8, \quad (22)$$

the expansion of the wave function was set to  $l=10$ .

K- point number is important and very efficient

When the elaborated overall energy of the crystal converges to be lower than  $10^{-2}mRy$  , the self-consistent estimations are reviewed to converge.

By using the second order derivative within WIEN2k code, the elastic constants are calculated.<sup>(43)</sup>

These approximations are widely used in WIEN2k package in order to obtain more accurate predictions of the electronic structure of the compounds. Which encourage scientific researchers to make studies on the material science.

### 3.3 Structural Properties

The crystal structure is the arrangement of atoms in the lattice, common crystal structures such as: cubic, hexagonal, and tetragonal, each influencing on the material behavior. Since the Heusler compounds are fcc.

The atoms coordinates in the unit cell determine the bonding interactions between the atoms.

In general, Materials show many structural properties, which play a role in their properties. These properties include, but not limited to the optimized lattice constant or lattice parameter, which denoted by (a).

It refers to the regular and steady distance between unit cells in a crystal lattice. It is one of the physical dimensions that determine the geometry of the unit cells in a crystal lattice.

(a) is an important factor characterizing the crystal structure of solids, denotes the unit cell edge's length. In addition to defining the angles between the borders, which in turn define the crystal's shape.

Also, the symmetry in the crystal keep the structure fixed and not varied, such as the rotation, and the reflection, they make the realization of solids to be simpler.

The bulk modulus (B) and its pressure derivative ( $B'$ ). The Bulk modulus of a substance can measure the resistance of the substance to bulk compression. B therefore symbolizes how resistant the material is to change and transform volume under compression that applicable on whole sides.

The lattice parameter (a), bulk modulus (B) and its pressure derivative ( $B'$ ) can be calculated by fitting the total energy to Murnaghan's equation of state (EOS), which is presented by:

$$E(V) = E_0 + \frac{BV}{B'} \left\{ \left( \frac{V_0}{V} \right)^{\frac{B'}{B-1}} + 1 \right\} - \frac{BV_0}{B-1} \quad (23)$$

Where P is the pressure =  $-\frac{dE}{dV}$  ,

B is the Bulk modulus,

$\dot{B}$  is the pressure derivative of bulk modulus

$$B' = -V \frac{dP}{dV} = V \frac{d^2E}{dV^2} \quad (24)$$

If (B) is negative, this means the volume decreases with increasing the applied pressure, this behavior is common for generality of materials.

As (B) increases, materials are less compressible and can make a high resistance against volume changes under applied pressure. On the contrary, materials with lower value of (B) are more compressible and their resistance against volume changes isn't high. <sup>(44)</sup>

In normal circumstances, the majority of materials almost have ( $\dot{B}$ ) with positive value which means, with decreasing pressure, the bulk modulus value decrease. And increasing pressure, the bulk modulus value increases. This phenomenon indicates that the materials are difficult and complicated to get compressible.

If ( $\dot{B}$ ) observed in a negative value, this implies that: with increasing the pressure, there will be decreasing in the bulk modulus. <sup>(44)</sup>

The normal Heusler has space group Fm-3m L21 (225) and inverse Heusler has space group Xa (216).

Full Heusler compounds have the formula  $X_2YZ$ , where X,Y, and Z denote a transition elements or an element from the main group. They are classified in the (fcc) structure, in which X and Y elements are occupied in the face centered positions, while Z atom is located at the body centered position. <sup>(1)</sup>

Or the inverse face centered cubic (ifcc) structure, the positions are reversed, as the X and Y are located at the body centered, and Z is positioned at face centered position.

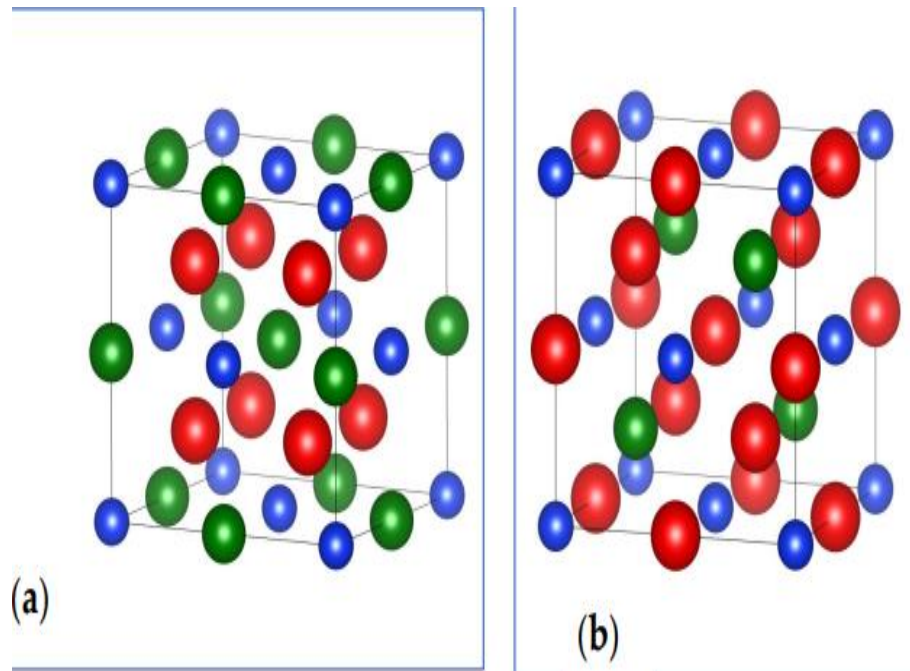
Heusler compounds have taken special attention because of their unique structure in which it makes a significant properties of these compounds in many sides like, the

electronic, the magnetic, and the elastic properties. So that the researchers prefer using Heusler compounds in many several applications.

Crystal structures of the full Heusler  $\text{Sc}_2\text{ZrAl}$  and  $\text{Sc}_2\text{ZrIn}$  compounds are displayed in figure (4).

**Figure 4**

*Crystal structures of  $\text{Sc}_2\text{ZrAl}$  and  $\text{Sc}_2\text{ZrIn}$  in (a) normal Heusler ( $L2_1$ ) and (b) inverse Heusler ( $Xa$ ) (Red: Sc, Green: Zr, Blue: Al/In)*



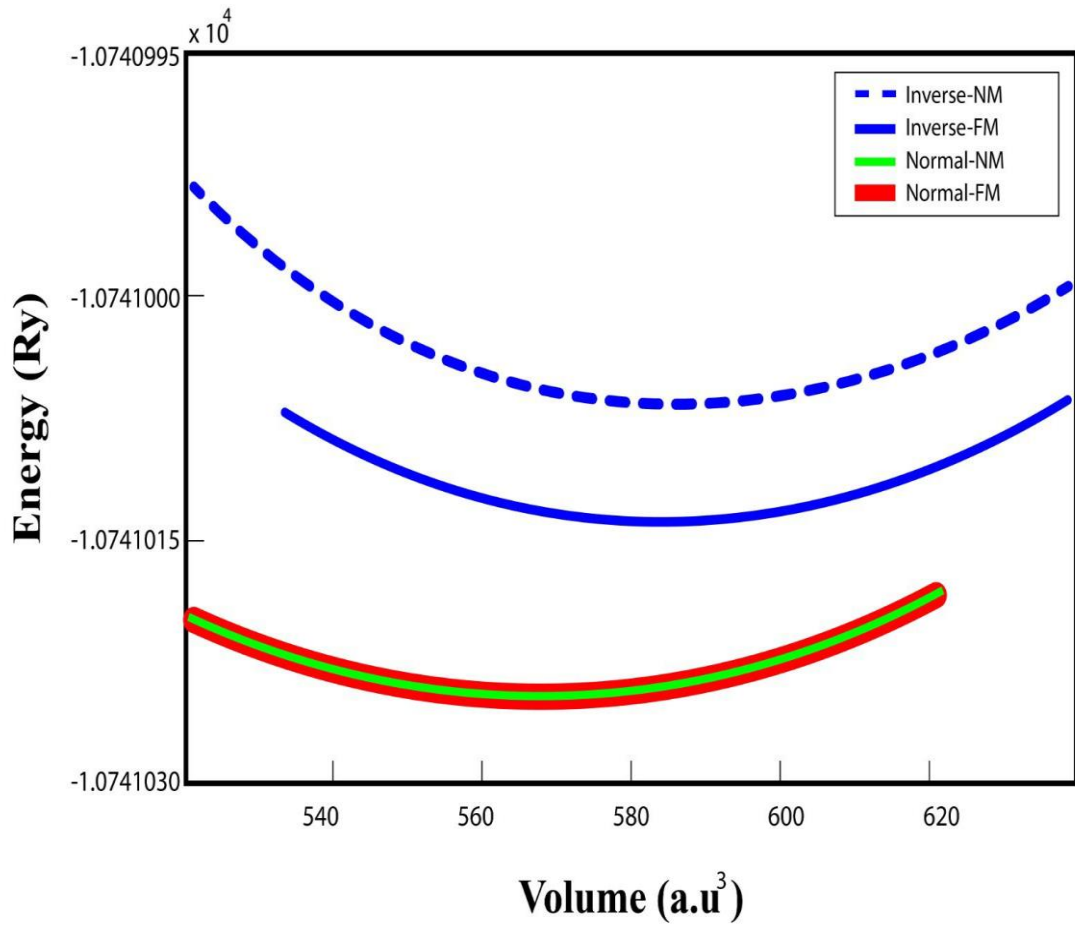
A guessed value of the lattice parameter was applied in the optimized volume calculation for each compound. (45)

Figures 5 and 6 show the overall energy against the volume of  $\text{Sc}_2\text{ZrAl}$  and  $\text{Sc}_2\text{ZrIn}$  alloys.

From these two figures we can clearly see the volume at which the energy is minimized, we can obviously see the stability of the material.

**Figure 5**

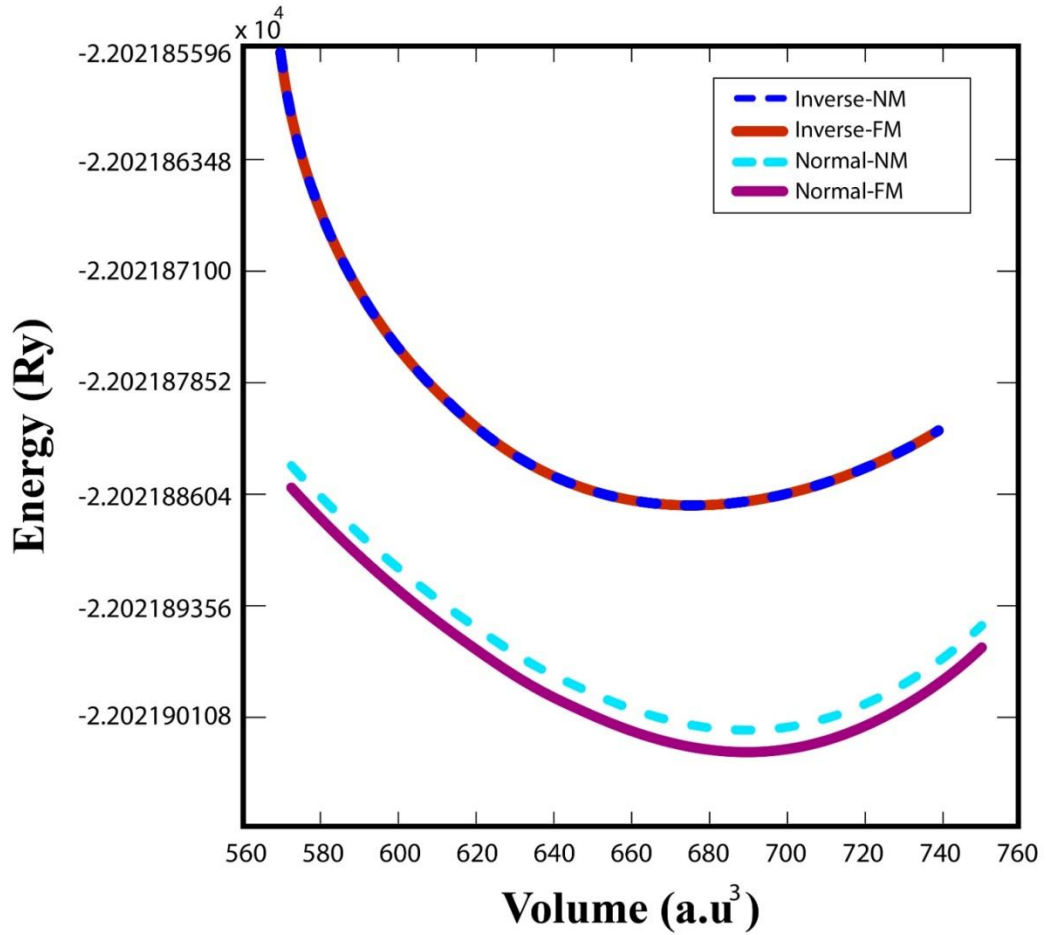
The overall energy ( $Ry$ ) versus volume ( $a.u.^3$ ) for both normal  $Sc_2ZrAl$  Heusler and inverse  $Sc_2ZrAl$  Heusler



It is clear from figure 5 that the normal  $Sc_2ZrAl$  has minimum energy  $E_0$  less than the inverse of  $Sc_2ZrAl$ , so the normal structure of  $Sc_2ZrAl$  is further mechanically stable and more balanced than the inverse structure of  $Sc_2ZrAl$ .

**Figure 6**

*The overall energy (Ry) versus volume ( $a.u.^3$ ) for normal  $Sc_2ZrIn$  Heusler and inverse  $Sc_2ZrIn$  Heusler*



likewise, from figure 6 it is obvious that the normal  $Sc_2ZrIn$  has minimum energy  $E_0$  less than the inverse of  $Sc_2ZrIn$ , so the normal structure of  $Sc_2ZrIn$  is greater mechanically stable and steady than the inverse structure of  $Sc_2ZrIn$ .

The structural properties (bulk modulus, lattice parameters and first pressure derivatives) of the full-Heusler  $Sc_2ZrAl$  and  $Sc_2ZrIn$  compounds were calculated from the equation of state (EOS) and listed in table 2.

**Table 2**

The lattice parameter ( $a$ ), bulk modulus ( $B$ ), its first derivative ( $\dot{B}$ ) and the minimum energy ( $E_0$ )

| Structure                | Space group                   | Reference           | A<br>( $\text{\AA}$ ) | B<br>(GPa) | $\dot{B}$<br>(GPa) | $E_0$<br>(Ry) |
|--------------------------|-------------------------------|---------------------|-----------------------|------------|--------------------|---------------|
| $\text{Sc}_2\text{ZrAl}$ | Fm-3m (225)<br>"normal case"  | Present             | 7.0281                | 72.89907   | 3.5578             | -10741.018925 |
|                          |                               | Theoretical<br>(45) | 7.02                  |            |                    |               |
|                          | F-43m (216)<br>"inverse case" | Present             | 6.9800                | 75.2563    | 3.3201             | -10741.025830 |
|                          |                               | Theoretical<br>(45) | 6.97                  |            |                    |               |
| $\text{Sc}_2\text{ZrIn}$ | Fm-3m (225)<br>"normal case"  | Present             | 7.1697                | 71.5755    | 4.6046             | -22021.901082 |
|                          |                               | Theoretical<br>(45) | 7.16                  |            |                    |               |
|                          | F-43m (216)<br>"inverse case" | Present             | 7.1372                | 73.5943    | 4.2894             | -22021.855960 |
|                          |                               | Theoretical<br>(45) | 7.14                  |            |                    |               |

From the data listed in this table, the calculated value of  $\text{Sc}_2\text{ZrAl}$  in the normal case is  $7.0281 \text{ \AA}$ , and for the inverse  $\text{Sc}_2\text{ZrAl}$  ( $a$ ) is equal  $6.98 \text{ \AA}$ .

For  $\text{Sc}_2\text{ZrIn}$  ( $a$ ) is equal  $7.1697 \text{ \AA}$  in the normal, and  $7.1372 \text{ \AA}$  in the inverse case.

These values are in a good agreement with the previous studies as listed in table (1).

### 3.4 Magnetic Properties

Heusler compounds show enchanting magnetic properties, so that Heusler compounds are classified as an important and interesting compounds for researchers to apply these compounds with their properties in many fascinating applications.

In this part, we have estimated the partial and total magnetic moment, the magnetic moment is identified as the magnetic strength and tendency to a magnet or else object that generate a magnetic field, for both normal and inverse Heusler  $\text{Sc}_2\text{ZrAl}$  and  $\text{Sc}_2\text{ZrIn}$  compounds.

The  $\text{MM}^{\text{tot}}$  for the normal  $\text{Sc}_2\text{ZrAl}$  was  $2.47675 \mu_B$  while it was  $0.01011$  for the inverse  $\text{Sc}_2\text{ZrAl}$ .

In the inverse structure it is less than the normal because of the small contribution of the Zr atom in the inverse case, while in normal case its contribution is larger.

So, one can note from the computed values of  $MM^{\text{tot}}$  for  $\text{Sc}_2\text{ZrAl}$  in the normal and inverse structures are close to the other theoretical values.<sup>(45)</sup>

Also, from table 3 one sees the outcomes for the normal and inverse Heusler.  $\text{Sc}_2\text{ZrIn}$  compounds. The  $MM^{\text{tot}}$  for the normal  $\text{Sc}_2\text{ZrIn}$  is higher because of the limited contribution of the Zr atom in the inverse situation.

In table 3 we compare the outcomes with other experimental and theoretical works.

**Table 3***Total, partial magnetic moment for inverse and normal Sc<sub>2</sub>ZrAl and Sc<sub>2</sub>ZrIn<sup>(45)</sup>*

| Structure                    | Ref.                        | Sc      | Sc      | Zr       | X        | Interstitial | MM <sup>tot</sup> |
|------------------------------|-----------------------------|---------|---------|----------|----------|--------------|-------------------|
| Normal Sc <sub>2</sub> ZrAl  | Present                     | 0.32961 | 0.32961 | 0.89927  | -0.01795 | 0.93621      | 2.47675           |
|                              | Theoretical <sup>[45]</sup> |         |         |          |          |              | 2.47              |
| Inverse Sc <sub>2</sub> ZrAl | Present                     | 0.00528 | 0.00477 | -0.00012 | -0.00408 | 0.00427      | 0.01011           |
|                              | Theoretical <sup>[45]</sup> |         |         |          |          |              | 0                 |
| Normal Sc <sub>2</sub> ZrIn  | Present                     | 0.34224 | 0.34224 | 0.93238  | 0.01747  | 1.01468      | 2.61407           |
|                              | Theoretical <sup>[45]</sup> |         |         |          |          |              | 2.66              |
| Inverse Sc <sub>2</sub> ZrIn | Present                     |         |         |          |          |              | 0.88333           |
|                              | Theoretical <sup>[45]</sup> | 0.24018 | 0.10369 | 0.20676  | -0.00453 | 0.33723      | 0.77              |

From table 3 we have found that the normal  $\text{Sc}_2\text{ZrAl}$  has non-integer total magnetic moment which means it has a ferromagnetic behavior.

But in the inverse  $\text{Sc}_2\text{ZrAl}$  Heusler compound has zero total magnetic moment, so it behaves as an antiferromagnetic compound.

On the other hand, for  $\text{Sc}_2\text{ZrIn}$  compound in the normal case the total magnetic moment is (2.61407) which means it has a ferromagnetic behavior.

While it has a small value in the inverse  $\text{Sc}_2\text{ZrIn}$  Heusler compound (0.88333) so that, it behaves as a ferrimagnet.

### **3.5 Electronic Properties**

The electronic properties are crucial properties that give the researchers much information about the compound behavior, and in turn the applications the compound can be utilized in.

In solid state physics, the electronic band structure or in short –band structure- describes the range of energy levels that electrons may have and probably not have (nicknamed as band gaps or forbidden bands).

The band structure (BS) and both of the partial and total density of states (PDOS, TDOS) are investigated in this section for both  $\text{Sc}_2\text{ZrAl}$  and  $\text{Sc}_2\text{ZrIn}$  compounds.

The investigation of the BS for normal Heusler compounds  $\text{Sc}_2\text{ZrAl}$  and  $\text{Sc}_2\text{ZrIn}$  are shown in the figures (7- 14), the pair spin-up and spin-down interiorly the GGA & mBJ methods.

**Table 4**

Energy band gap of normal and inverse of  $Sc_2ZrAl$ , and  $Sc_2ZrIn$  utilizing PBE-GGA and mBJ potentials

| Compound           | Spin      | Band gap type | PBE-GGA $E_g$ | mBJ $E_g$ |
|--------------------|-----------|---------------|---------------|-----------|
| Normal $Sc_2ZrAl$  | Spin up   | —             | Metal         | Metal     |
|                    | Spin down | —             | Metal         | Metal     |
| Inverse $Sc_2ZrAl$ | Spin up   | —             | Metal         | Metal     |
|                    | Spin down | —             | Metal         | Metal     |
| Normal $Sc_2ZrIn$  | Spin up   | —             | Metal         | Metal     |
|                    | Spin down | —             | Metal         | Metal     |
| Inverse $Sc_2ZrIn$ | Spin up   | —             | Metal         | Metal     |
|                    | Spin down | —             | Metal         | Metal     |

**Figure 7**

The band structure for normal  $Sc_2ZrAl$  Heusler compound by employing PBE-GGA method for (a) spin down normal Heusler compound, (b) spin up normal Heusler compound.

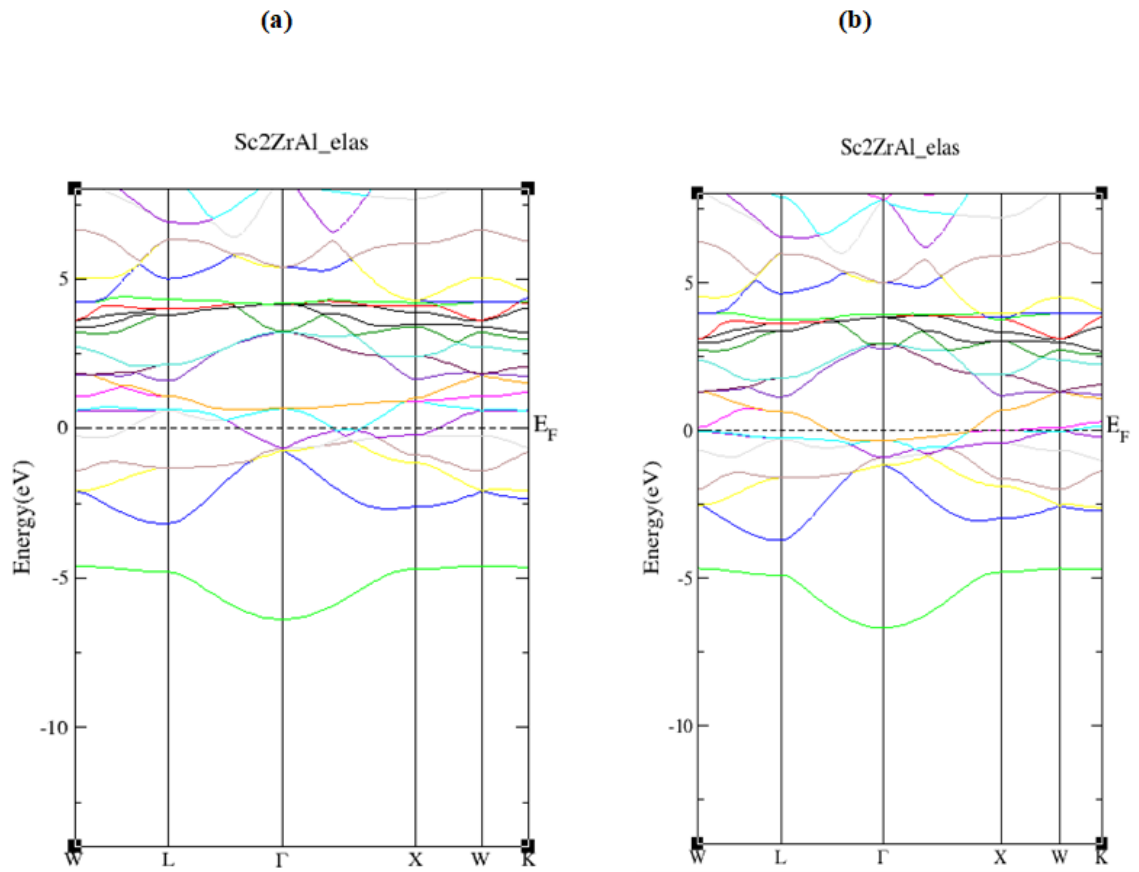


Figure 7 (a) presents the metallic attitude of the spin down band structure, by using the GGA method for the normal- Heusler  $\text{Sc}_2\text{ZrAl}$  compound with zero energy gap.

Figure 7 (b) presents the metallic attitude of the spin up band structure, by using the GGA method for the normal- Heusler  $\text{Sc}_2\text{ZrAl}$  compound with zero energy gap.

**Figure 8**

*The band structure for inverse  $\text{Sc}_2\text{ZrAl}$  Heusler compound by using PBE-GGA method for (a) spin down inverse Heusler compound (b) spin up inverse Heusler compound*

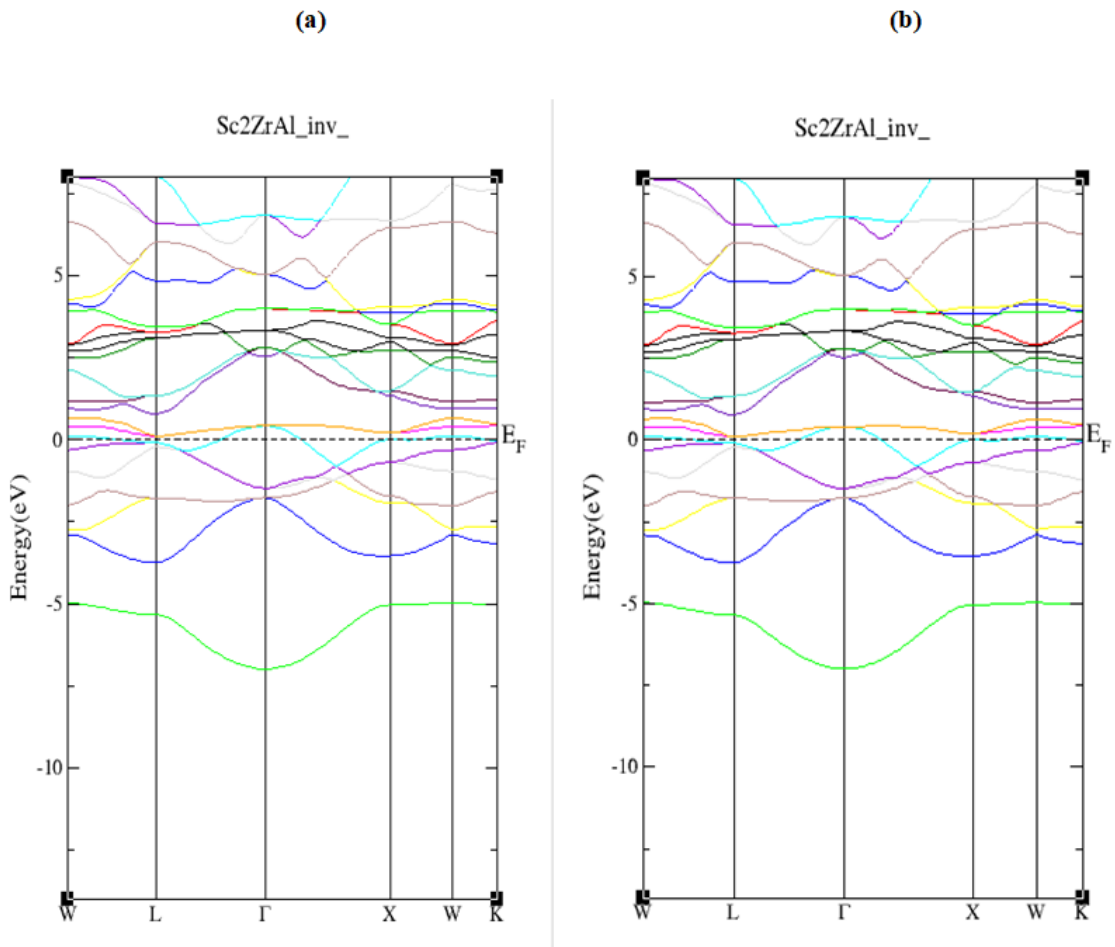
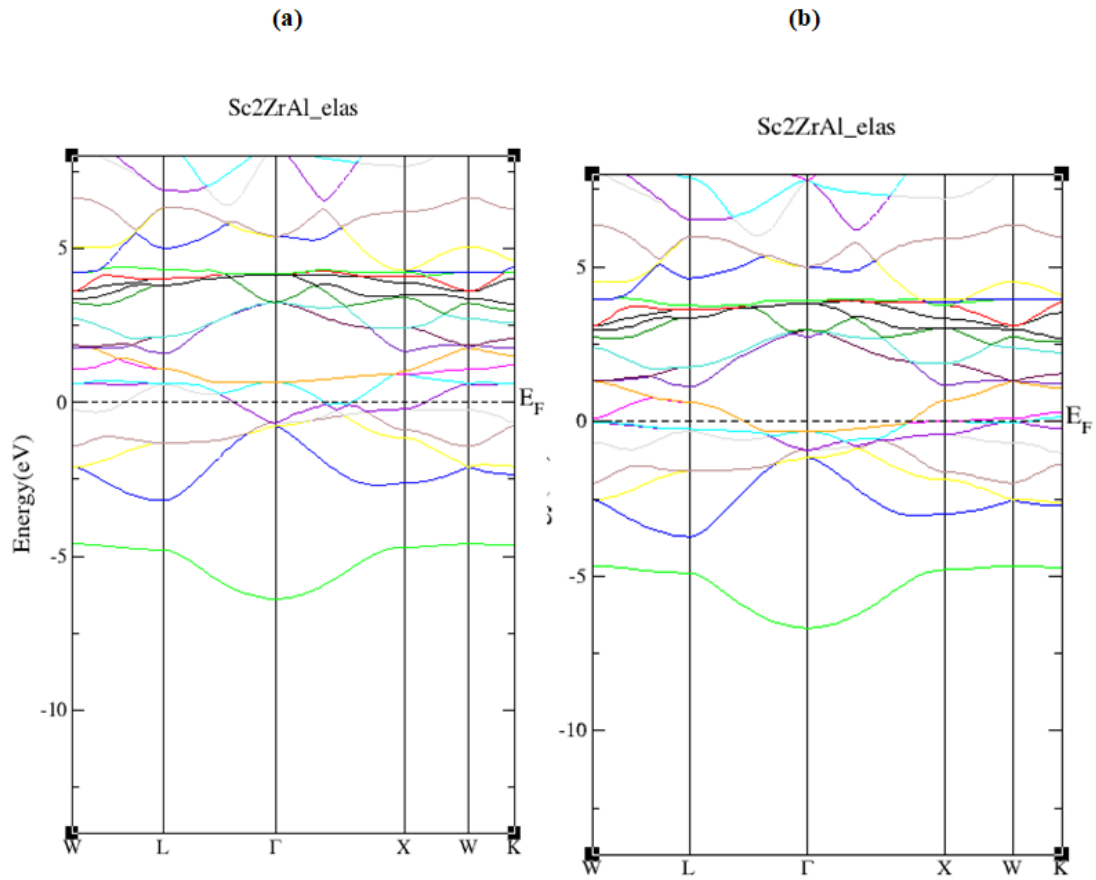


Figure 8 (a) presents metallic attitude of the spin down band structure, by using the GGA method for inverse Heusler  $\text{Sc}_2\text{ZrAl}$  compound with zero energy gap.

Figure 8 (b) presents metallic attitude of the spin up band structures, by using the GGA method for inverse Heusler  $\text{Sc}_2\text{ZrAl}$  compound with zero energy gap.

**Figure 9**

The band structure for normal  $\text{Sc}_2\text{ZrAl}$  Heusler compound by using mBJ-GGA method for (a) spin down normal Heusler compound (b) spin up normal Heusler compound



mBJ-GGA method shows in figure 9 (a) the metallic behavior of the spin down band structure, for normal- Heusler  $\text{Sc}_2\text{ZrAl}$  compound with zero energy gap.

mBJ-GGA method shows in figure 9 (b) the metallic behavior of the spin up band structure, for normal- Heusler  $\text{Sc}_2\text{ZrAl}$  compound with zero energy gap.

**Figure 10**

The band structure for inverse  $Sc_2ZrAl$  Heusler compound by using mbj method for (a) spin down regular Heusler compound (b) spin up regular Heusler compound

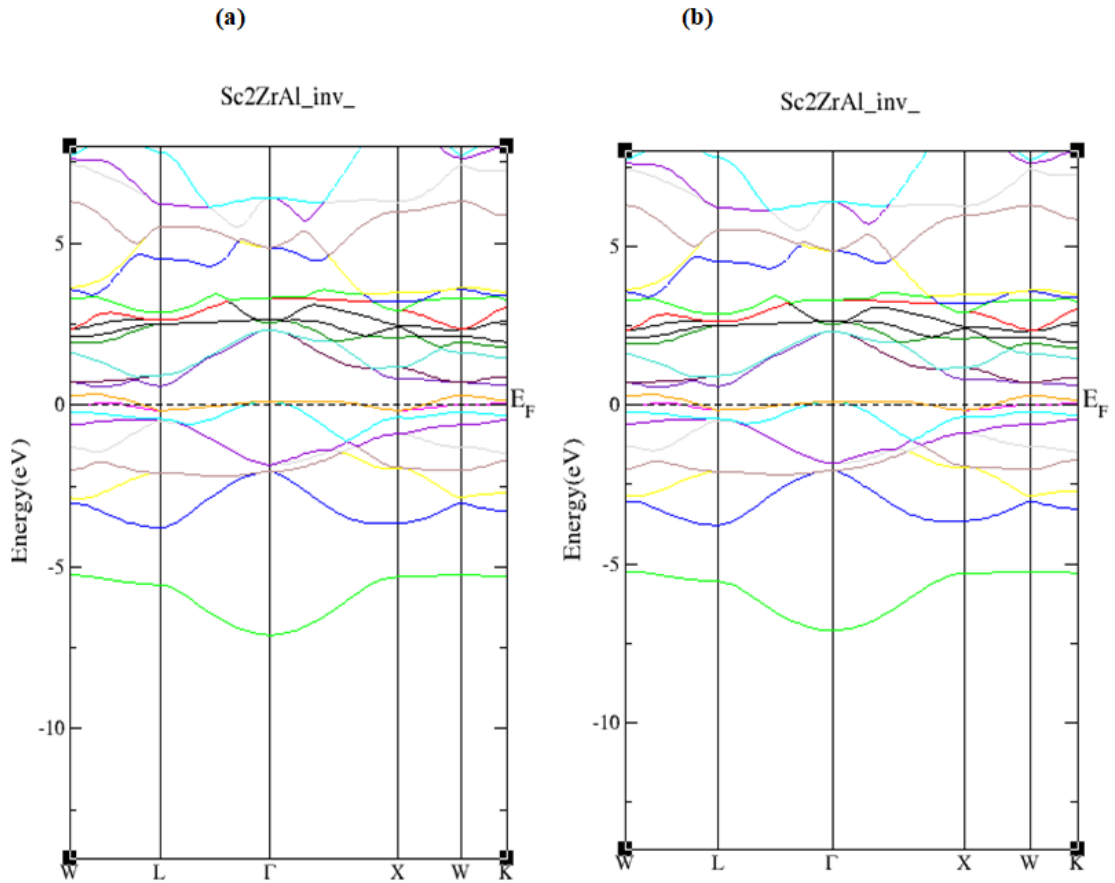


Figure 10 (a) shows metallic behavior of the spin down band structures, within mBJ-GGA method for inverse Heusler  $Sc_2ZrAl$  compound with zero energy gap.

Figure 10 (b) shows metallic behavior of the spin up band structures, within mBJ-GGA method for inverse Heusler  $Sc_2ZrAl$  compound with zero energy gap.

Figure 11 (a) presents the metallic attitude of the spin down band structure, by utilizing the GGA method for normal- Heusler  $Sc_2ZrIn$  compound with zero energy gap.

Figure 11 (b) presents the metallic attitude of the spin up band structures, by utilizing the GGA method for normal- Heusler  $Sc_2ZrIn$  compound with zero energy gap.

Likewise, figure 12 (a) presents the metallic attitude of the spin down band structure, among employing the GGA method for inverse Heusler  $\text{Sc}_2\text{ZrIn}$  compound with zero energy gap.

Figure 12 (b) presents the metallic attitude of the spin up band structure, among employing the GGA method for inverse Heusler  $\text{Sc}_2\text{ZrIn}$  compound with zero energy gap.

Figure 13 (a) presents the metallic attitude of the spin down band structures, by employing the mBJ method for normal- Heusler  $\text{Sc}_2\text{ZrIn}$  compound with zero energy gap.

Figure 13 (b) presents the metallic attitude of the spin up band structures, by employing the mBJ method for normal Heusler  $\text{Sc}_2\text{ZrIn}$  compound with zero energy gap.

Figure 14 (a) presents the metallic attitude of the spin down band structures, within mBJ method for inverse Heusler  $\text{Sc}_2\text{ZrIn}$  compound with zero energy gap.

Figure 14 (b) presents the metallic behavior of the spin up band structures, by employing the mBJ method for inverse Heusler  $\text{Sc}_2\text{ZrIn}$  compound with zero energy gap.

Figures (15-22) show the total and partial density of states for spin up and spin down for inverse and normal Heusler  $\text{Sc}_2\text{ZrAl}$  and  $\text{Sc}_2\text{ZrIn}$  Heusler compounds. Density of states in figures (15-22) show the metallic behavior for both  $\text{Sc}_2\text{ZrAl}$  and  $\text{Sc}_2\text{ZrIn}$ .

### **3.6 Elastic properties**

In this section, some constants and ratios are studied for the normal and inverse Heusler ( $\text{Sc}_2\text{ZrAl}$ ,  $\text{Sc}_2\text{ZrIn}$ ) compounds, as follows:

The bulk modulus (B) as we mentioned in the previous sections, B estimate and quantify the ability and the talent of the substance to resist and hold against the applied pressure.

Shear modulus (S), which is called also the rigidity modulus, it measures the ratio between the shear stress and the shear strain. So we can be knowledgeable on the solid's behavior under external forces and loads.

Bugh ratio (B/S), Poisson's ratio, measures the ratio between the side strain" its direction is perpendicular to the applied and practiced external force" and the longitudinal strain "its direction is the same as the applied force". So it can be possible to determine the expansion happens in the solids in the direction that is perpendicular to the external force.

Young's modulus (Y) is a quantity that estimates the stiffness of the materials. It's the stress's ratio to the strain, (Y) helps in characterizing the mechanical behavior of solids.

Anisotropic factor (A), this factor is very usable in describing the solid's elastic properties change with the directions.

The specifications mechanical stability for the cubic crystal are: <sup>(46-48)</sup>

$$C_{11} > 0,$$

$$C_{44} > 0,$$

$$C_{11} + 2 C_{12} > 0,$$

$$C_{11} - C_{12} > 0,$$

$$C_{11} > B > C_{12}.$$

Where the bulk  $C_{44}$  – shear, and the tetragonal shear moduli,  $C'$ , must be positive. <sup>(49)</sup>

The third criterion  $C_{11} + 2 C_{12}$  is known as the spinodal pressure,  $p_s$ ,

While the fourth criterion is used to define an additional elastic constant which called the tetragonal shear modulus:

$$C' = C_{11} - C_{12} \quad (25)$$

Tetragonal stability is achieved when the hydrostatic pressure becomes  $2p > C'$ .

The Cauchy pressure for cubic crystal is given by the relation: <sup>(49)</sup>

$$P_s = C_{12} - C_{44} \quad (26)$$

Originating from the examined compounds and the mechanical stability circumstances that pointed out above, our calculations for the normal and inverse Heusler Sc<sub>2</sub>ZrAl and Sc<sub>2</sub>ZrIn compounds are listed in table (5).

Sc<sub>2</sub>ZrAl is stable in the normal case, and unstable in the inverse case, Sc<sub>2</sub>ZrIn is also stable in the normal case and unstable in the inverse case.

To evaluate shear modulus and the Bulk modulus we have used Voigt approximation.<sup>(50)</sup>

Voigt shear modulus  $S_v$  can be calculated by:

$$S_v = \frac{1}{5} (C_{11} - C_{12} + 3C_{44}) \quad (27)$$

While the Bulk modulus for the cubic structure is donated by:<sup>(50)</sup>

$$B = \frac{1}{3} (C_{11} + 2C_{12}) \quad (28)$$

Young modulus (Y) is the ratio between stress to strain:

$$Y = \frac{9 B S_v}{(S_v + 3B)} \quad (29)$$

Anisotropic factor is given by:

$$A = \frac{2C_{44}}{C_{11} - C_{12}} \quad (30)$$

Poisson's ratio is donated by:

$$\nu = \frac{3B - 2S_v}{2(3B + S_v)} \quad \text{or} \quad \frac{C_{12}}{C_{11} + C_{12}} \quad (31)$$

**Table 5**

*The elastic constants ( $C_{ij}$ ), bulk modulus ( $B$ ), and anisotropic factor ( $A$ ) of  $Sc_2ZrAl$  and  $Sc_2ZrIn$*

| Compound   | $C_{11}$ (GPa) | $C_{12}$ (GPa) | $C_{44}$ (GPa) | $B$ (GPa) | $A$     |
|------------|----------------|----------------|----------------|-----------|---------|
| Normal     |                |                |                |           |         |
| $Sc_2ZrAl$ | 84.893         | 67.369         | 59.447         | 72.89907  | 6.784   |
| Inverse    |                |                |                |           |         |
| $Sc_2ZrAl$ | 47.935         | 73.698         | 55.954         | 75.2563   | -4.343  |
| Normal     |                |                |                |           |         |
| $Sc_2ZrIn$ | 83.4457        | 64.3059        | 55.0630        | 71.5755   | 5.7537  |
| Inverse    |                |                |                |           |         |
| $Sc_2ZrIn$ | 46.191         | 83.716         | 55.580         | 73.5943   | -2.9622 |

The  $B / S$  ratio determine the ductility and brittleness of the materials since the hardness, the solidity, and the rigidity of materials are quantified by the Bulk modulus ( $B$ ) and shear modulus ( $S$ ).

If  $B / S$  ratio  $>1.75$  and  $\nu > 0.26$  , the material is in a ductile nature. Otherwise, materials behave as a brittle nature.

The nature of bonding is indicated by the  $\nu$  value. Compounds with covalent bonds have a  $\nu$  value smaller than 0.25, while for compounds with ionic bonds, the  $\nu$  value is between 0.25 and 0.5. <sup>(47-49)</sup>

The Young modulus ( $Y$ ) measures the stiffness of the materials, as the value of the Young modulus increases, the stiffness increases.

These calculations were performed on the stable compounds, which are normal  $Sc_2ZrAl$  and normal  $Sc_2ZrIn$ .

Our results are tabulated in table (6):

**Table 6**

*Bulk modulus ( $B$ ), Shear modulus ( $S$ ),  $B/S$  ratio, Voigt Poisson's ratio ( $\nu$ ), and Young's modulus ( $Y$ ) of normal  $Sc_2ZrAl$  and normal  $Sc_2ZrIn$  compounds*

| Compound   | $B$ (GPa) | $S$ (GPa) | $B/S$ | $\nu$ | $Y$ (GPa) |
|------------|-----------|-----------|-------|-------|-----------|
| normal     |           |           |       |       |           |
| $Sc_2ZrAl$ | 72.89907  | 39.173    | 1.86  | 0.272 | 99.66     |
| normal     |           |           |       |       |           |
| $Sc_2ZrIn$ | 71.5755   | 36.86576  | 1.94  | 0.280 | 94.39     |

Our calculations for B/S ratio is 1.86 for the normal  $\text{Sc}_2\text{ZrAl}$ , which means it's ductile. Also, it is 1.94 for the normal  $\text{Sc}_2\text{ZrIn}$ , so it is ductile.

Both compounds (normal  $\text{Sc}_2\text{ZrAl}$  and normal  $\text{Sc}_2\text{ZrIn}$ ) are with ionic bonds since their  $v$  value is greater than 0.25

## Chapter Four

### Discussions and Conclusions

Studying full Heusler compounds can supply awesome information into the various properties of the compounds and their applications in many different fields.

In this thesis, structural, magnetic, electronic, and elastic properties of normal and inverse full-Heusler ( $\text{Sc}_2\text{ZrAl}$ ,  $\text{Sc}_2\text{ZrIn}$ ) compounds were studied. It becomes clearer and more obvious that the full Heusler compounds we have studied are showing an attractive and glamorous behavior that make these compounds very useful and effective in many fields, as they are promising to be the most efficient item in the future of technology.

The results are summarized as follows:

From the structural properties of the compounds, and from graphing the energy versus volume of both compounds, in  $\text{Sc}_2\text{ZrAl}$  case the compound in normal case is more stable than the inverse one.

Also from graphing  $\text{Sc}_2\text{ZrIn}$  is also more stable in the normal case than the inverse case since the energy is minimized.

According to the magnetic properties, the compound  $\text{Sc}_2\text{ZrAl}$  in the normal case is ferromagnetic and antiferromagnetic in the inverse case since it has a total magnetic moment  $MM^{\text{tot}}$  2.47675 and 0.01011 in the normal and inverse case respectively.

While the compound  $\text{Sc}_2\text{ZrIn}$  is ferromagnetic in the normal case with total magnetic moment  $MM^{\text{tot}} = 2.61407$  and ferrimagnet in the inverse case with  $MM^{\text{tot}} = 0.88333$ .

In addition, according to the electronic band structure calculations these compounds normal Heusler  $\text{Sc}_2\text{ZrAl}$ , inverse Heusler  $\text{Sc}_2\text{ZrAl}$ , normal Heusler  $\text{Sc}_2\text{ZrIn}$  and inverse Heusler  $\text{Sc}_2\text{ZrIn}$  are metals with zero-energy band gaps in both GGA and mBJ methods.

As for the elastic properties, it emphasized that both normal Heusler  $\text{Sc}_2\text{ZrAl}$  and normal Heusler  $\text{Sc}_2\text{ZrIn}$  are stable. While inverse Heusler  $\text{Sc}_2\text{ZrAl}$  and inverse Heusler  $\text{Sc}_2\text{ZrIn}$  are unstable.

The B/S ratio showed that both compounds normal Heusler  $\text{Sc}_2\text{ZrAl}$  and normal Heusler  $\text{Sc}_2\text{ZrIn}$  are ductile, since its value is  $> 1.75$ , it was 1.86 for normal  $\text{Sc}_2\text{ZrAl}$ , and 1.94 for the normal  $\text{Sc}_2\text{ZrIn}$ .

And from the  $\nu$  value (greater than 0.25) for the two compounds, it was 0.272 and 0.280 for  $\text{Sc}_2\text{ZrAl}$  and  $\text{Sc}_2\text{ZrIn}$  in the normal case, respectively. They are with ionic bonds.

Furthermore, this thesis with its results blazed the trail in front of other optimizations on Heusler compounds, Scientists and researchers are now able to continue studying the translating the properties of these compounds into many applications and useful devices.

## List of Abbreviations

| Abbreviation     | Meaning   |
|------------------|---|
| FP-LAPW          | Full potential linearized augmented plane wave. |
| DFT              | Density functional theory                       |
| GGA              | Generalized gradient approximation              |
| mBJ              | Modified Becke Johnson                          |
| DOS              | Density of state                                |
| BS               | Band structure                                  |
| LDA              | Local density approximation                     |
| BOA              | Born Oppenheimer approximation.                 |
| APW              | Augmented plane wave.                           |
| LAPW             | Linearized augmented plane wave.                |
| SGSs             | Spin-gapless semiconductors                     |
| SMA <sub>s</sub> | Shape memory alloys                             |
| SE               | Schrodinger equation                            |
| H                | Hamiltonian                                     |
| E                | Energy  |
| $\Psi$           | Wave function                                   |
| BZ               | Brillion Zone                                   |
| IBZ              | Irreducible Brillion zone                       |
| R <sub>MT</sub>  | Muffin-tin radii                                |
| Fcc              | Face centered cubic                             |
| ifcc             | Inverse face centered cubic                     |
| MM               | Magnetic moment                                 |
| PDOS             | Partial density of states                       |
| TDOS             | Total density of states                         |

## References

- (1) Palmstrøm CJ. Heusler compounds and spintronics. *Progress in Crystal Growth and Characterization of Materials* [Internet]. 2016 Jun [cited 2024 May 7];62(2):371–97. Available from: <https://linkinghub.elsevier.com/retrieve/pii/S0960897416300237>
- (2) Martinolich AJ, Neilson JR. Toward Reaction-by-Design: Achieving Kinetic Control of Solid State Chemistry with Metathesis. *Chem Mater* [Internet]. 2017 Jan 24 [cited 2024 May 7];29(2):479–89. Available from: <https://pubs.acs.org/doi/10.1021/acs.chemmater.6b04861>
- (3) Galanakis I, Mavropoulos P, Dederichs PH. Electronic structure and Slater–Pauling behaviour in half-metallic Heusler alloys calculated from first principles. *J Phys D: Appl Phys* [Internet]. 2006 Feb [cited 2024 May 1];39(5):765. Available from: <https://dx.doi.org/10.1088/0022-3727/39/5/S01>
- (4) Arshad H, Zafar M, Ahmad S, Rizwan M, Khan MI, Gillani SSA, et al. Theoretical study of structural, electronic and magnetic properties of equiatomic quaternary CoPdCrZ (Z = Si, Ge, P) Heusler alloys. *Mod Phys Lett B* [Internet]. 2019 Nov 10 [cited 2024 May 1];33(31):1950389. Available from: <https://www.worldscientific.com/doi/abs/10.1142/S0217984919503895>
- (5) Elphick K, Frost W, Samiepour M, Kubota T, Takanashi K, Sukegawa H, et al. Heusler alloys for spintronic devices: review on recent development and future perspectives. *Science and Technology of Advanced Materials* [Internet]. 2021 Dec 31 [cited 2024 May 1];22(1):235–71. Available from: <https://www.tandfonline.com/doi/full/10.1080/14686996.2020.1812364>
- (6) Aray Y, Rodriguez J, Vega D. An implementation of the atoms in molecules theory to the FPLAPW method. *Computer Physics Communications* [Internet]. 2002 Mar [cited 2024 May 7];143(3):199–212. Available from: <https://linkinghub.elsevier.com/retrieve/pii/S0010465501004283>
- (7) Zhang M, Liu Z, Hu H, et al. Is Heusler compound Co<sub>2</sub>CrAl a half-metallic ferromagnetic band structure, and transport properties *Magnetism and Magnetic Materials*. 2004;277:130–5.

- (8) Özdogan K, Galanakis I. First-principles electronic and magnetic properties of the half-metallic antiferromagnet  $\text{Cr}_2\text{MnSb}$ . Journal of Magnetism and Magnetic Materials [Internet]. 2009 Aug 1 [cited 2024 May 1];321(15):L34–6. Available from: <https://www.sciencedirect.com/science/article/pii/S0304885309000225>
- (9) Hakimi M, Kameli P, Salamati H. Structural and magnetic properties of Heusler alloys prepared by mechanical alloying, Magnetism and Magnetic Materials. 2010;
- (10) Abu-Jafar MS, Abu-Labdeh AM, El-Hasan M. The energy band gap of ScN in the rocksalt phase obtained with LDA/GGA+USIC approximations in FP-LAPW method. Computational Materials Science [Internet]. 2010 Dec [cited 2024 May 7];50(2):269–73. Available from: <https://linkinghub.elsevier.com/retrieve/pii/S092702561000409X>
- (11) Galanakis I. Theory of Heusler and Full-Heusler Compounds. In: Felser C, Hirohata A, editors. Heusler Alloys [Internet]. Cham: Springer International Publishing; 2016 [cited 2024 May 8]. p. 3–36. (Springer Series in Materials Science; vol. 222). Available from: [https://link.springer.com/10.1007/978-3-319-21449-8\\_1](https://link.springer.com/10.1007/978-3-319-21449-8_1)
- (12) Hirohata A, Huminiuc T, Sinclair J, Wu H, Samiepour M, Vallejo-Fernandez G, et al. Development of antiferromagnetic Heusler alloys for the replacement of iridium as a critically raw material. J Phys D: Appl Phys [Internet]. 2017 Sep [cited 2024 May 1];50(44):443001. Available from: <https://dx.doi.org/10.1088/1361-6463/aa88f4>
- (13) Boudali A, Zemouli M, Saadaoui F, Khodja MD. Structural, Elastic, Electronic, and Magnetic Properties of the Full-Heusler Compounds  $\text{Ti}_2\text{NiX}$  (X= Al, Ga, and In). J Supercond Nov Magn [Internet]. 2017 Jan [cited 2024 May 7];30(1):15–23. Available from: <http://link.springer.com/10.1007/s10948-016-3707-8>
- (14) Hayashi K, Li H, Eguchi M, Nagashima Y, Miyazaki Y. Magnetic Full-Heusler Compounds for Thermoelectric Applications. In: Ranjan Sahu D, N. Stavrou V, editors. Magnetic Materials and Magnetic Levitation [Internet]. IntechOpen; 2021 [cited 2024 May 7]. Available from:

<https://www.intechopen.com/books/magnetic-materials-and-magnetic-levitation/magnetic-full-heusler-compounds-for-thermoelectric-applications>

- (15) Abu Baker D, Abu-Jafar M, Mousa A, Jaradat R, Ilaiwi K, Khenata R. Structural, magnetic, electronic and elastic properties of half-metallic ferromagnetism full-Heusler alloys: Normal-  $\text{Co}_2\text{TiSn}$  and inverse-  $\text{Z RhGa}$  using FP-LAPW method. *Materials Chemistry and Physics*. 2020;
- (16) Abu-Jafar MS, Leonhardi V, Jaradat R, Mousa AA, Al-Qaisi S, Mahmoud NT, et al. Structural, electronic, mechanical, and dynamical properties of scandium carbide. *Results in Physics* [Internet]. 2021 Feb [cited 2024 May 7];21:103804. Available from: <https://linkinghub.elsevier.com/retrieve/pii/S2211379720322105>
- (17) Wakeel M, Murtaza G, Ullah H, Khan S, Laref A, Ameer Z, et al. Structural, electronic, and magnetic properties of palladium based full Heusler compounds: DFT study. *Physica B: Condensed Matter* [Internet]. 2021 May [cited 2024 May 7];608:412716. Available from: <https://linkinghub.elsevier.com/retrieve/pii/S0921452620306967>
- (18) Wei Q, Zhang R, Zhang M, Zhang Y, Cao L, Zhang J. Three new Ag-based full-Heusler alloys:  $\text{Ag}_2\text{TiGa}$ ,  $\text{Ag}_2\text{VGa}$ , and  $\text{Ag}_2\text{TiTi}$ . *ChemPhysMater* [Internet]. 2022 Jul [cited 2024 May 7];1(3):211–8. Available from: <https://linkinghub.elsevier.com/retrieve/pii/S2772571522000146>
- (19) Al-Masri Kh, Abu-Jafar M, Farout M. Structural, magnetic, electronic and elastic properties of the full-Heusler compounds  $\text{Sc}_2\text{TiAl}$ ,  $\text{Sc}_2\text{TiSi}$  using FP-LAPW method. *Materials Chemistry and Physics*. 2022;
- (20) Yahya SJ, Abu-Jafar MS, Al Azar S, Mousa AA, Khenata R, Abu-Baker D, et al. The Structural, Electronic, Magnetic and Elastic Properties of Full-Heusler  $\text{Co}_2\text{CrAl}$  and  $\text{Cr}_2\text{MnSb}$ : An Ab Initio Study. *Crystals* [Internet]. 2022 Nov 6 [cited 2024 May 3];12(11):1580. Available from: <https://www.mdpi.com/2073-4352/12/11/1580>
- (21) Alnafie Y, Kumar R. Structure optimization and electronic properties of full Heusler  $\text{Fe}_2\text{NbIn}$  and half Heusler  $\text{FeNbIn}$ . In Chitkara University, Himachal Pradesh, India; 2022 [cited 2024 May 7]. p. 020057. Available from: <https://pubs.aip.org/aip/acp/article/2824215>

- (22) Cherifa Horimek, Gueddouh A, Belkhir ML. Physical properties of full and half Heusler alloys  $\text{Co}_2\text{CrAl}$  and  $\text{CoCrSb}$ . First principal study. 2022 [cited 2024 May 7]; Available from: <https://rgdoi.net/10.13140/RG.2.2.21097.16488>
- (23) Mualla Z, Abu-Jafar MS, Bassalat A, Abualrob H, Mousa AA, Manzoor M, et al. Structural, electronic, and elastic properties of RbI using the FP-LAPW method. *Mod Phys Lett B* [Internet]. 2023 Nov 10 [cited 2024 May 7];37(31):2350145. Available from: <https://www.worldscientific.com/doi/10.1142/S0217984923501452>
- (24) Jaradat RT, Abu-Jafar MS, Farout M, Azar SM, Khenata R, Mousa AA. Structural, electronic, magnetic, and optical investigations of sodium chalcogenides: First-principles calculations. *AIP Advances* [Internet]. 2023 Jan 1 [cited 2024 May 7];13(1):015110. Available from: <https://pubs.aip.org/adv/article/13/1/015110/2871211/Structural-electronic-magnetic-and-optical>
- (25) Kervan N. Electronic structure, magnetic and optical properties of the  $\text{Ti}_2\text{RuAl}$  full-Heusler compound by a first-principles study. *Eur Phys J B* [Internet]. 2023 Jul [cited 2024 May 7];96(7):106. Available from: <https://link.springer.com/10.1140/epjb/s10051-023-00570-7>
- (26) Singh P, Mahla S, Chaudhary MG, Agrawal R, Singh C, Verma AS. Structural, electronic, optical, mechanical and magnetic properties of  $\text{Co}_2\text{CrZ}$  ( $Z = \text{As, B, Ga, Pb}$ ) full-Heusler compounds. *JOR* [Internet]. 2023 Aug [cited 2024 May 7];19(4):387–99. Available from: [https://chalcogen.ro/387\\_SinghP.pdf](https://chalcogen.ro/387_SinghP.pdf)
- (27) Jabar A, Bahmad L, Benyoussef S. Study of physical properties of the quaternary full-Heusler alloy:  $\text{FeMnCuSi}$ . *Journal of Alloys and Compounds* [Internet]. 2023 Jun [cited 2024 May 7];947:169604. Available from: <https://linkinghub.elsevier.com/retrieve/pii/S0925838823009076>
- (28) Ain QU, Qaid SMH, Yousaf M, Alkadi M, Iqbal AB, Ahmed AAA, et al. A promising optoelectronic and thermoelectric response of full Heusler  $\text{Na}_2\text{TlX}$  ( $X = \text{Bi, Sb}$ ) alloys: a DFT approach. *Phys Scr* [Internet]. 2023 Nov 1 [cited 2024 May 7];98(11):115920. Available from: <https://iopscience.iop.org/article/10.1088/1402-4896/acfd7>

- (29) Kapil J, Shukla P, Pathak A. A DFT+U Based Study of Full-Heusler Alloy Ru<sub>2</sub>VSi. *Macromolecular Symposia* [Internet]. 2023 Feb [cited 2024 May 7];407(1):2100420. Available from: <https://onlinelibrary.wiley.com/doi/10.1002/masy.202100420>
- (30) Abbes C, Belbachir S, Abbassa H, Meskine S, Boukortt A. Exploring the structural, electronic, optical properties and stability of Na<sub>2</sub>SrX (Si and Ge) full-Heusler alloys: A first principle investigation. *emergent mater* [Internet]. 2023 Aug [cited 2024 May 7];6(4):1319–27. Available from: <https://link.springer.com/10.1007/s42247-023-00523-x>
- (31) Ait Elkoua I, Masrouf R. Investigation of structural, electronic, magnetic, and mechanical stability of a non-trivial topology phase in compound full-Heusler alloys TiHfFe X (X=Al, Ga, In). *Mod Phys Lett B* [Internet]. 2024 Jan 27 [cited 2024 May 7];2450187. Available from: <https://www.worldscientific.com/doi/10.1142/S0217984924501872>
- (32) Fernández FM. The Born-Oppenheimer approximation. 2019 [cited 2024 May 7]; Available from: <http://rgdoi.net/10.13140/RG.2.2.21650.91840>
- (33) Cottenier S. Density Functional Theory and the family of (L) APW-methods: a step-by-step introduction. *Instituut voor Kern-en Stralingsfysica, KU Leuven, Belgium*. 2002;4(0):41.
- (34) Fabrizio M. Hartree-Fock Approximation. In: *A Course in Quantum Many-Body Theory* [Internet]. Cham: Springer International Publishing; 2022 [cited 2024 May 7]. p. 81–120. (Graduate Texts in Physics). Available from: [https://link.springer.com/10.1007/978-3-031-16305-0\\_3](https://link.springer.com/10.1007/978-3-031-16305-0_3)
- (35) Sholl DS, Steckel JA. *Density functional theory: a practical introduction*. Second edition. Hoboken, NJ: Wiley; 2022.
- (36) Blaha P, Schwarz K, Madsen GK, Kvasnicka D, Luitz J. *Wien2k*. An augmented plane wave + local orbitals program for calculating crystal properties. 2001;60.
- (37) Bechstedt F. Kohn-Sham Scheme. In: *Many-Body Approach to Electronic Excitations* [Internet]. Berlin, Heidelberg: Springer Berlin Heidelberg; 2015 [cited 2024 May 7]. p. 89–104. (Springer Series in Solid-State Sciences; vol. 181). Available from: [https://link.springer.com/10.1007/978-3-662-44593-8\\_6](https://link.springer.com/10.1007/978-3-662-44593-8_6)

- (38) Kohn W, Sham LJ. Self-Consistent Equations Including Exchange and Correlation Effects. *Phys Rev* [Internet]. 1965 Nov 15 [cited 2024 May 7];140(4A):A1133–8. Available from: <https://link.aps.org/doi/10.1103/PhysRev.140.A1133>
- (39) Bulgac A, Yu Y. SUPERFLUID LDA (SLDA): LOCAL DENSITY APPROXIMATION FOR SYSTEMS WITH SUPERFLUID CORRELATIONS. *Int J Mod Phys E* [Internet]. 2004 Feb [cited 2024 May 7];13(01):147–56. Available from: <https://www.worldscientific.com/doi/abs/10.1142/S0218301304001874>
- (40) Zahariev F, Leang SS, Gordon MS. Functional derivatives of meta-generalized gradient approximation (meta-GGA) type exchange-correlation density functionals. *The Journal of Chemical Physics* [Internet]. 2013 Jun 28 [cited 2024 May 7];138(24):244108. Available from: <https://pubs.aip.org/jcp/article/138/24/244108/594362/Functional-derivatives-of-meta-generalized>
- (41) Tran F, Blaha P, Schwarz K. Band gap calculations with Becke–Johnson exchange potential. *J Phys: Condens Matter* [Internet]. 2007 May 16 [cited 2024 May 7];19(19):196208. Available from: <https://iopscience.iop.org/article/10.1088/0953-8984/19/19/196208>
- (42) Blaha P, Schwarz K, Madsen G, Kvasnicka D, Luitz J. WIEN2k. Technical Universitat Wien, Austria; 2001.
- (43) I Relast Package is Provided by M. Jamal as Part of the Commercial Code WIEN2K. Available online. 2014 [cited 2023 Jan 5]; Available from: <http://www.wien2k.at/>
- (44) Murnaghan FD. The Compressibility of Media under Extreme Pressures. *Proceedings of the National Academy of Sciences of the United States of America*. 1944;30(9):244–7.
- (45) Hana Y, Chenb Z, Kuanga M, Liuc Z, Wangd X, Wang X. Scandium-based full Heusler compounds: A comprehensive study of competition between XA and L21 atomic ordering. 171AD;

- (46) Born M, Huang K. Dynamical Theory of Crystal Lattices. Am J Phys. 1956;23:474.
- (47) Gupta Y, Sinha M, Verma S. Exploring the structural, elastic, lattice dynamical stability and thermoelectric properties of semiconducting novel quaternary Heusler alloy LiScPdPb. J Solid State Chem. 2021;304:122601.
- (48) Abu-Jafar M, Dayton-Oxland R, Jaradat R, Mousa A, Khenata R. Structural, electronic, mechanical and elastic properties of Scandium Chalcogenides by first-principles calculations. Phase. 2020;93:773.
- (49) Wu SC, Fecher GH, Naghavi SS, Felser C. Elastic properties and stability of Heusler compounds: Cubic Co<sub>2</sub>YZ compounds with L2<sub>1</sub> structure. J Appl Phys. 2019;125:082523.
- (50) Hill R. The Elastic Behaviour of a Crystalline Aggregate. Proc Phys Soc. 1952;65:349.

# Appendices

## Appendix A

### Figures of Study

**Figure 11**

*The band structure for normal  $Sc_2ZrIn$  Heusler compound by using GGA method for (a) spin down normal Heusler compound (b) spin up normal Heusler compound*

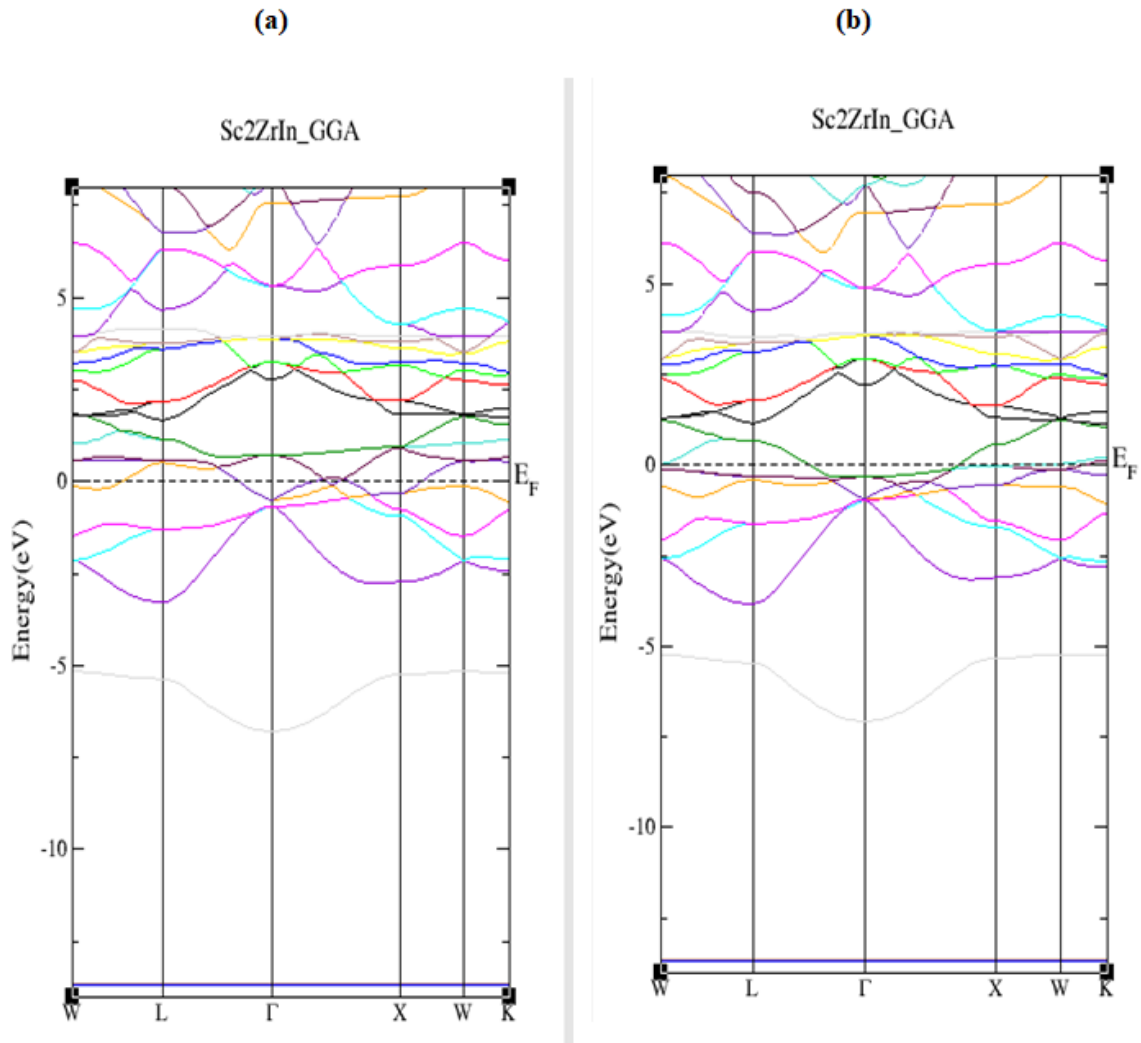


**Figure 12**

The band structure for inverse  $Sc_2ZrIn$  Heusler compound by using GGA method for (a) spin down regular Heusler compound (b) spin up regular Heusler compound

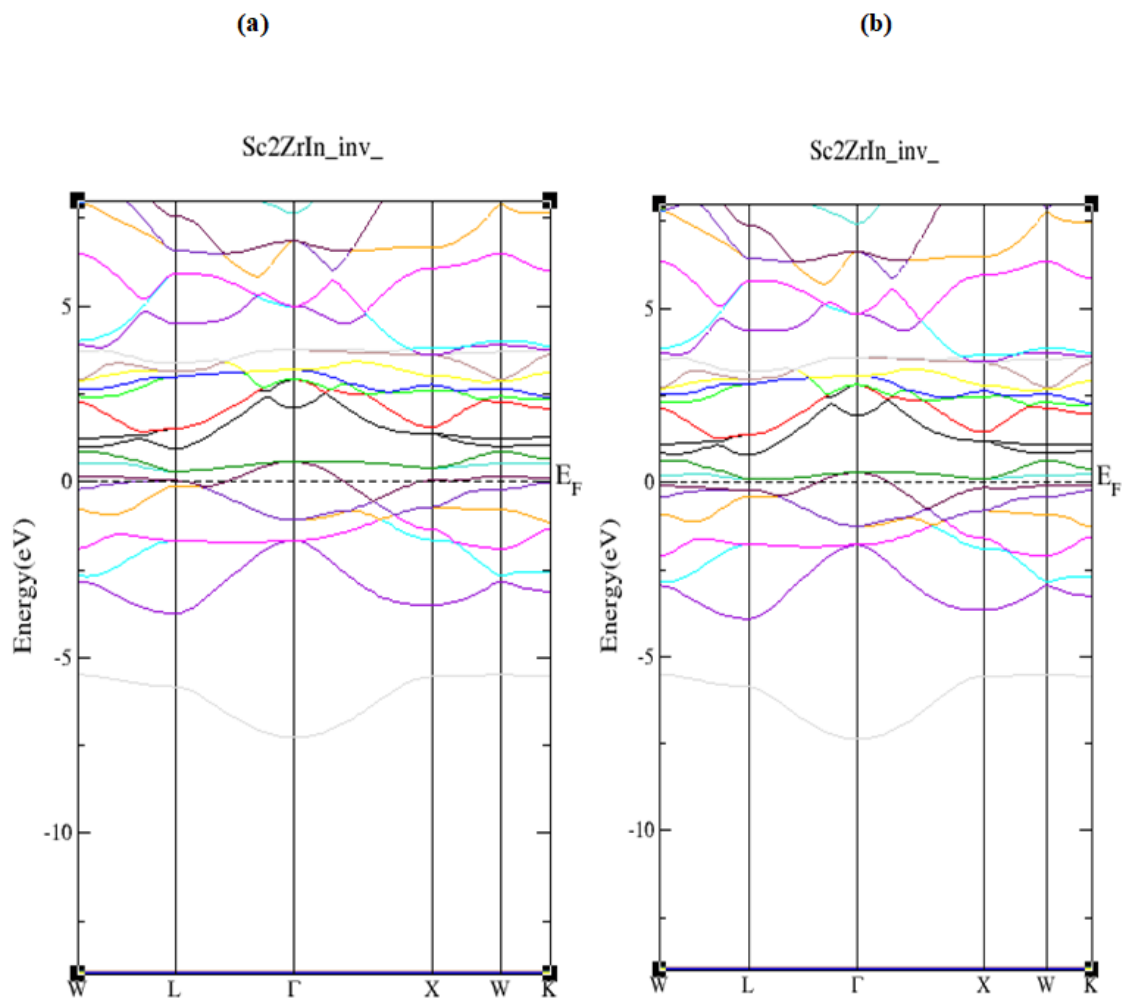


**Figure 13**

The band structure for normal  $Sc_2ZrIn$  Heusler compound by using mBJ method for (a) spin down normal Heusler compound, (b) spin up normal Heusler compound

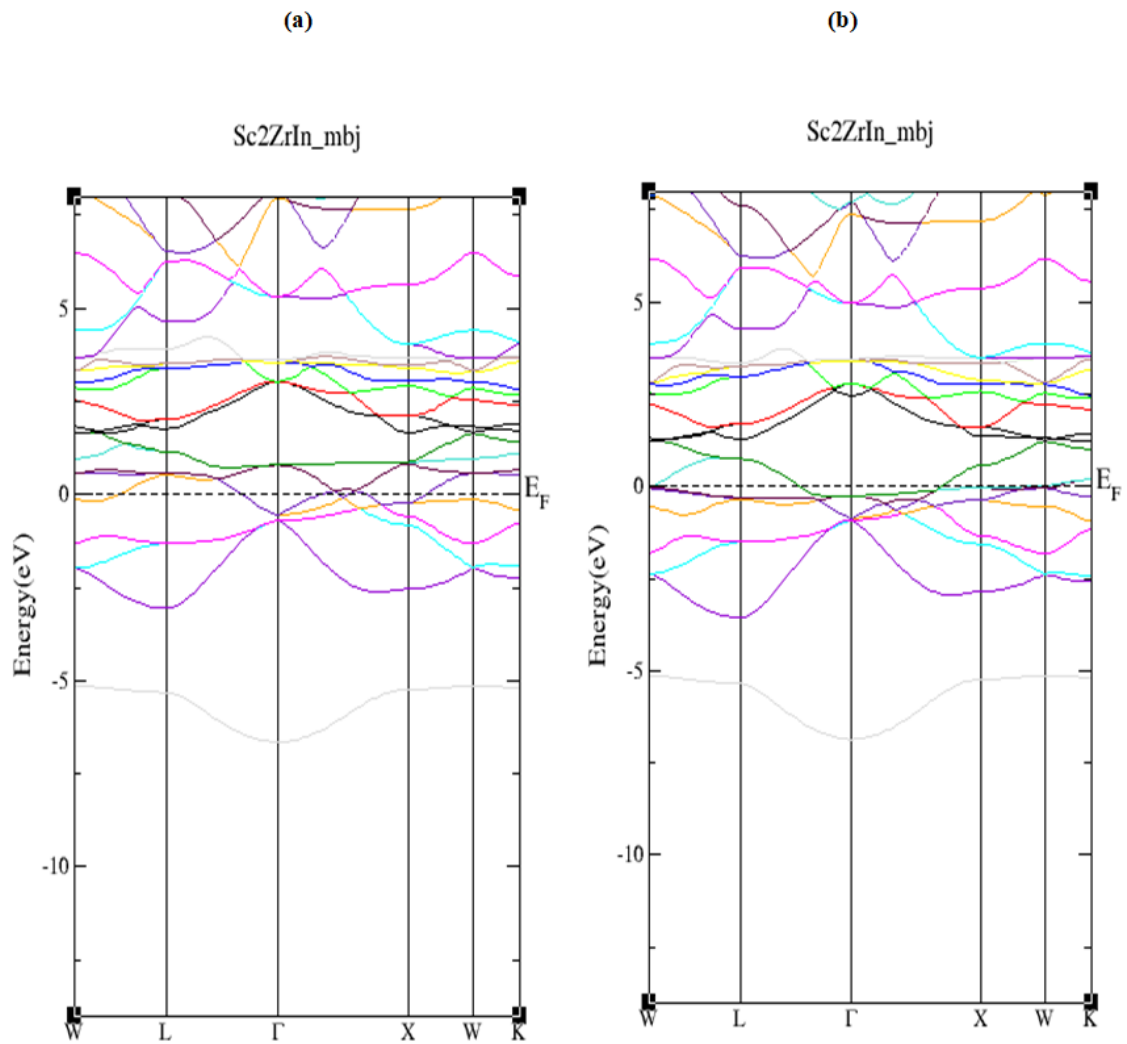


**Figure 14**

The band structure for inverse  $Sc_2ZrIn$  Heusler compound by using mBJ method for (a) spin down normal Heusler compound, (b) spin up normal Heusler compound

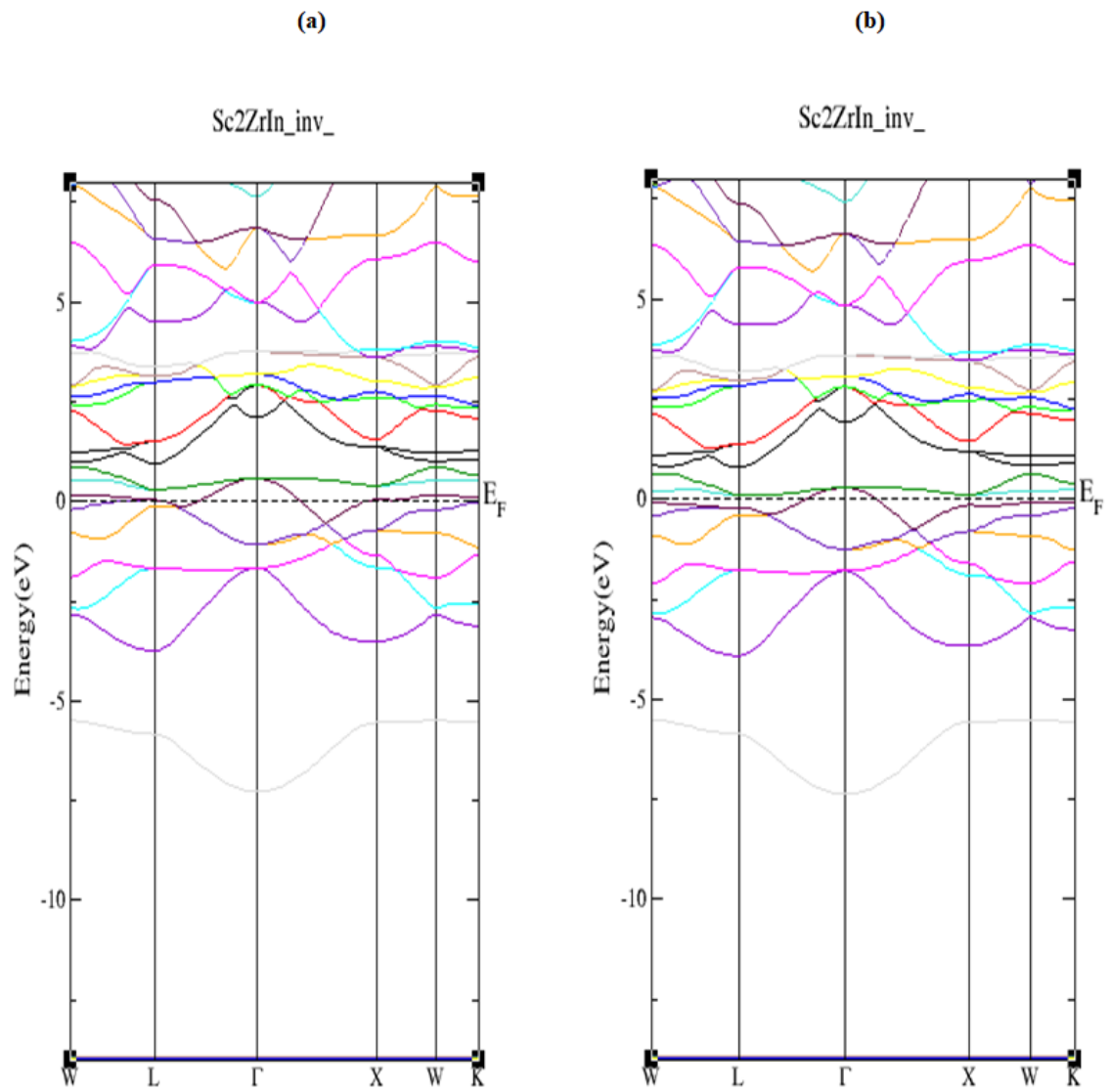


**Figure 15**

(a) Total density of states of spin up and spin down for normal  $Sc_2ZrAl$  and partial density of states of spin up and spin down for (b) Sc atom (c) Zr atom (d) Al atom of normal compound using GGA method

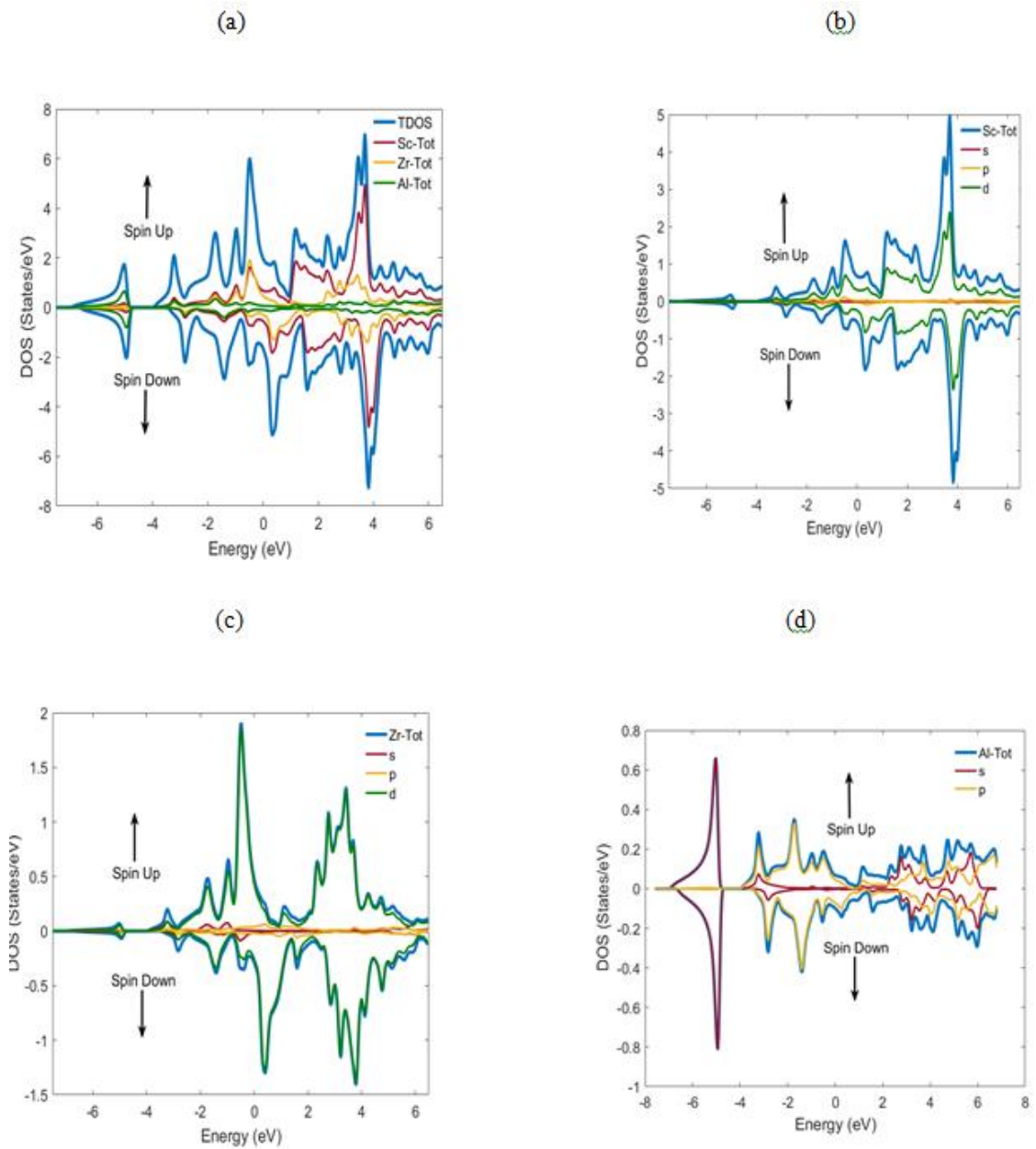


**Figure 16**

(a) Total density of states of spin up and spin down for normal  $Sc_2ZrAl$  and partial density of states of spin up and spin down for (b) Sc atom (c) Zr atom (d) Al atom of normal compound using mBJ method

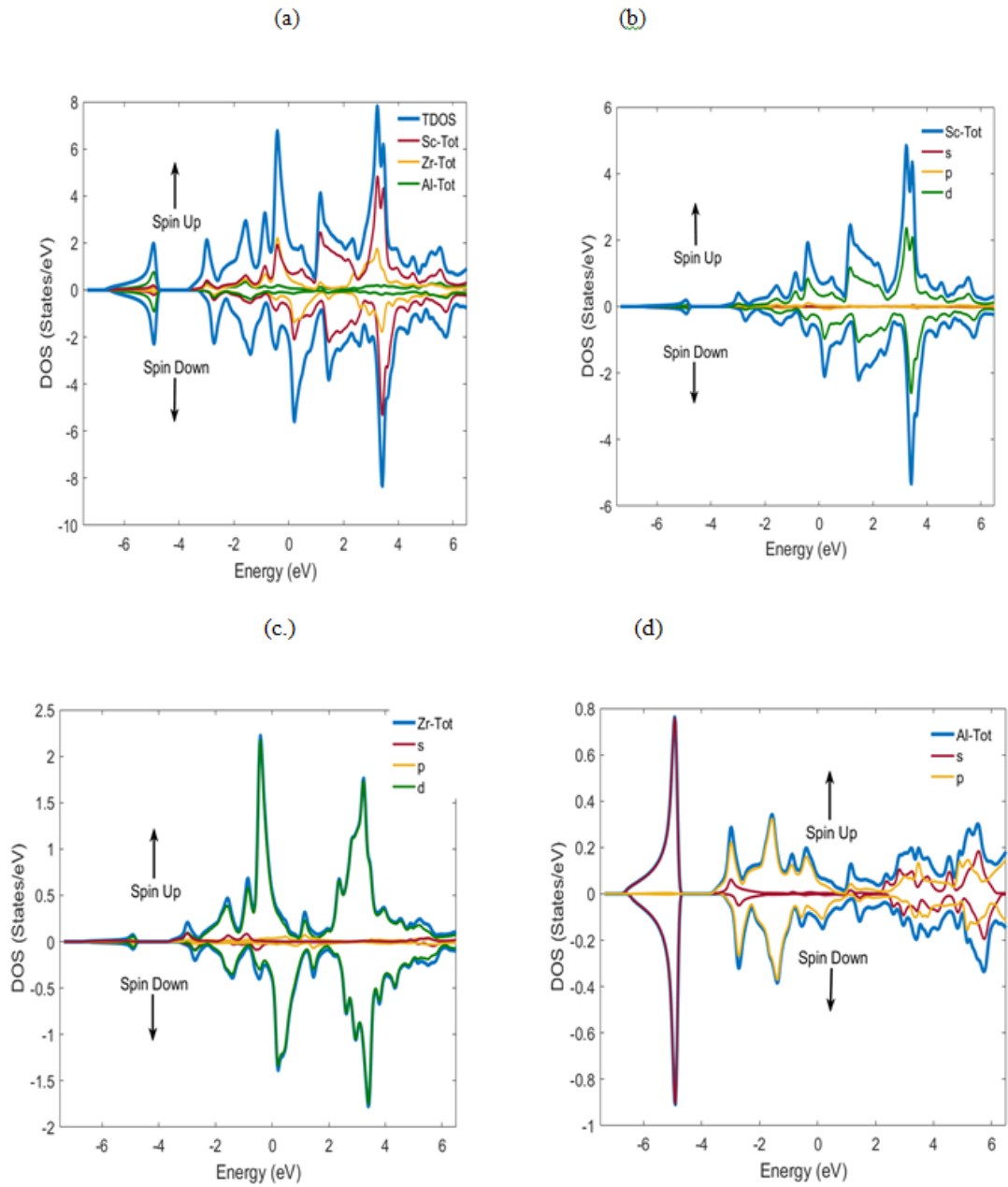


**Figure 17**

(a) Total density of states of spin up and spin down for inverse  $Sc_2ZrAl$  and partial density of states of spin up and spin down for (b) Sc1 atom (c) Sc2 atom (d) Zr atom (e) Al atom of inverse compound using GGA method

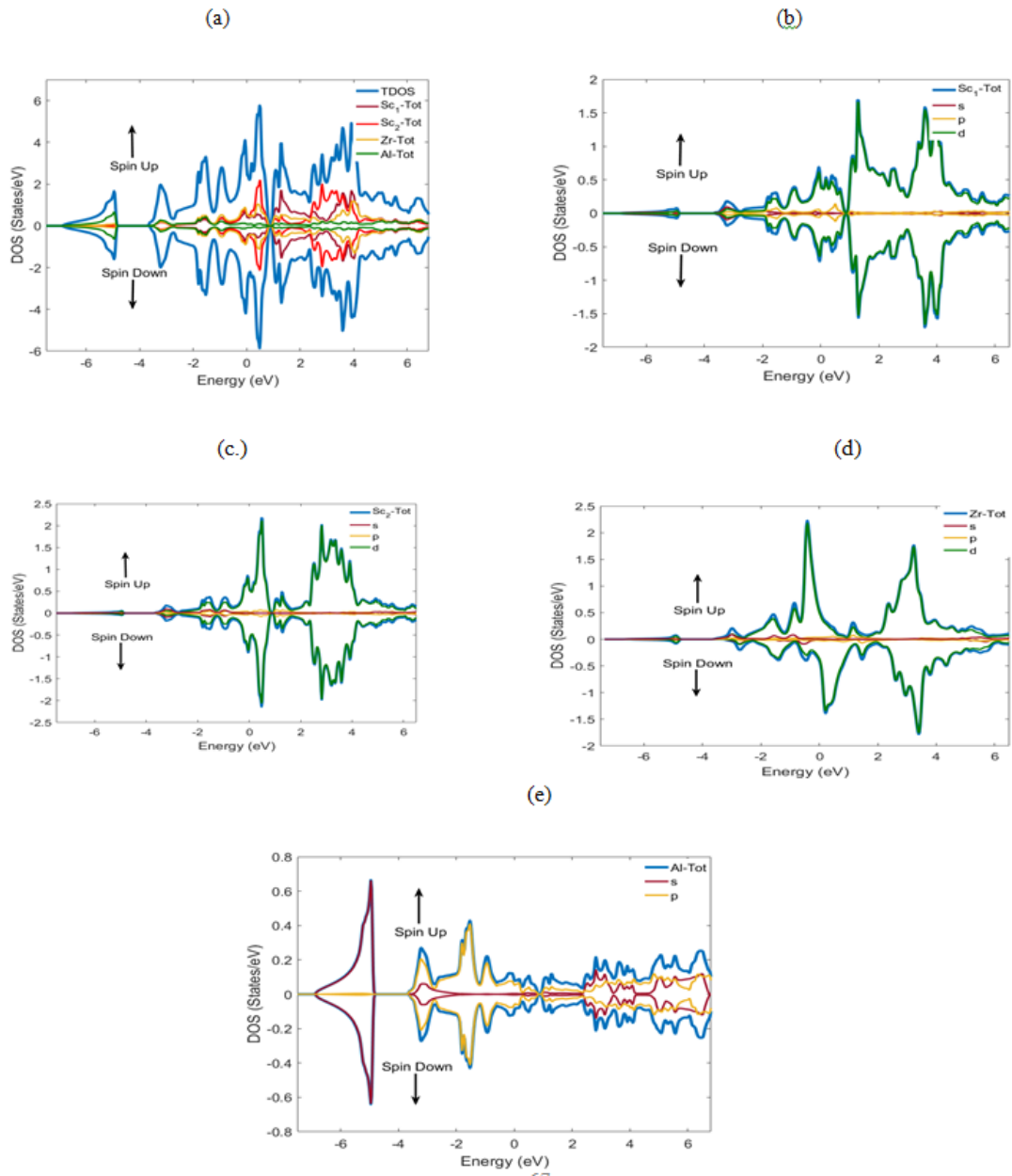


**Figure 18**

(a) Total density of states of spin up and spin down for inverse  $Sc_2ZrAl$  and partial density of states of spin up and spin down for (b) Sc1 atom (c) Sc2 atom (d) Zr atom (e) Al atom of normal compound using mBJ method

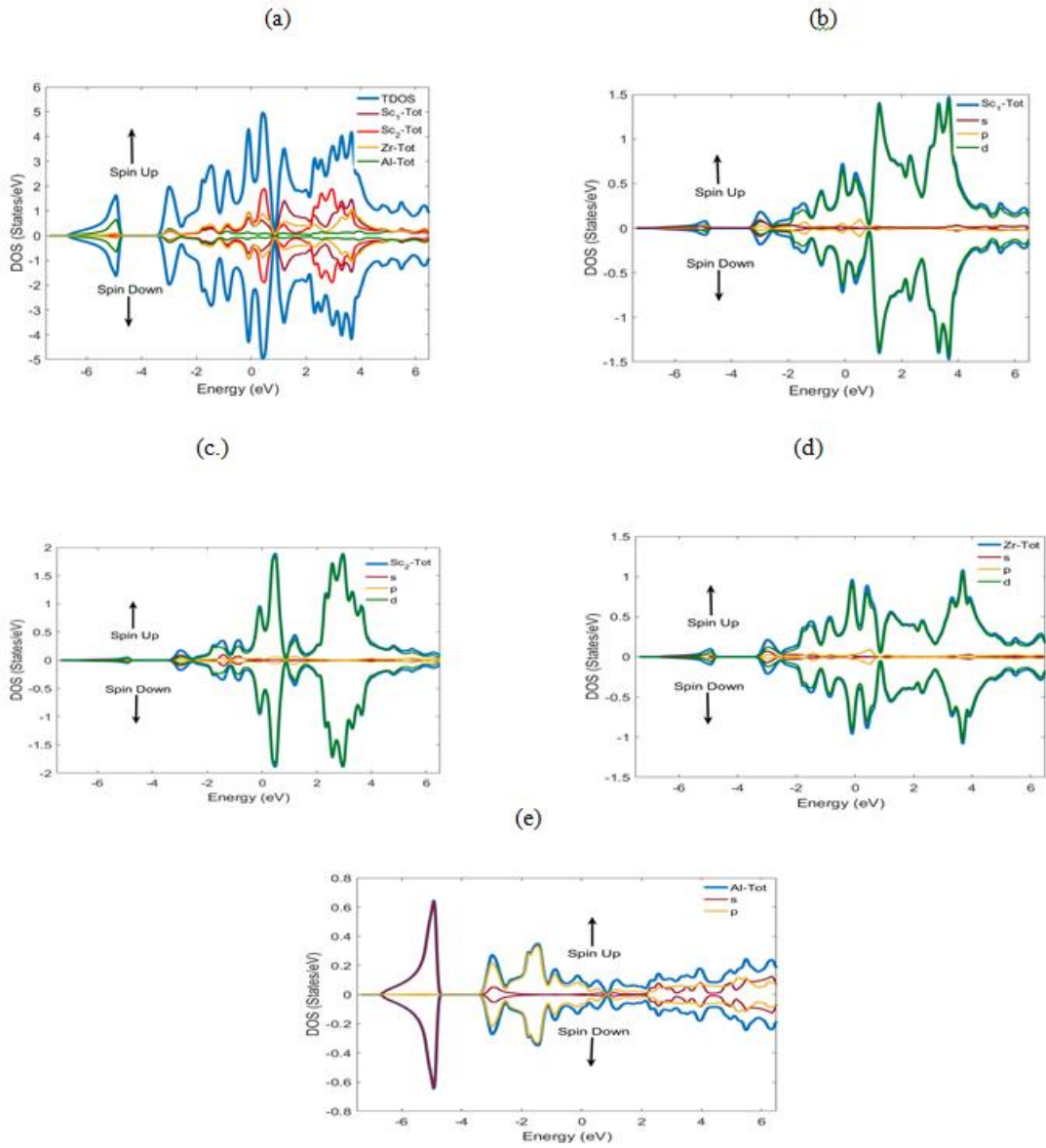


**Figure 19**

(a) Total density of states of spin up and spin down for normal  $\text{Sc}_2\text{ZrIn}$  and partial density of states of spin up and spin down for (b) Sc atom (c) Zr atom (d) In atom of normal compound using GGA method

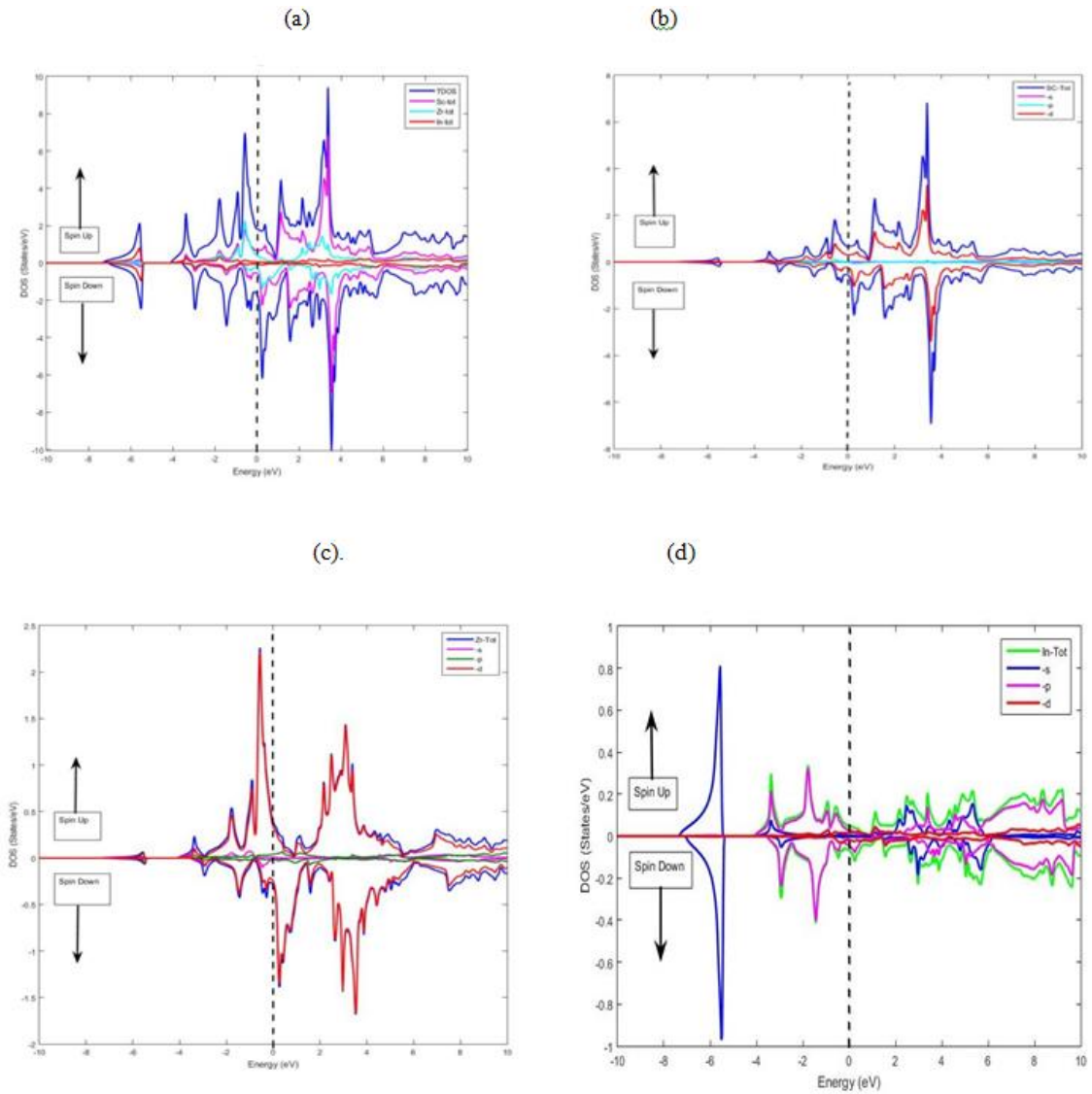


**Figure 20**

(a) Total density of states of spin up and spin down for normal  $\text{Sc}_2\text{ZrIn}$  and partial density of states of spin up and spin down for (b) Sc atom (c) Zr atom (d) In atom of normal compound using mBJ method

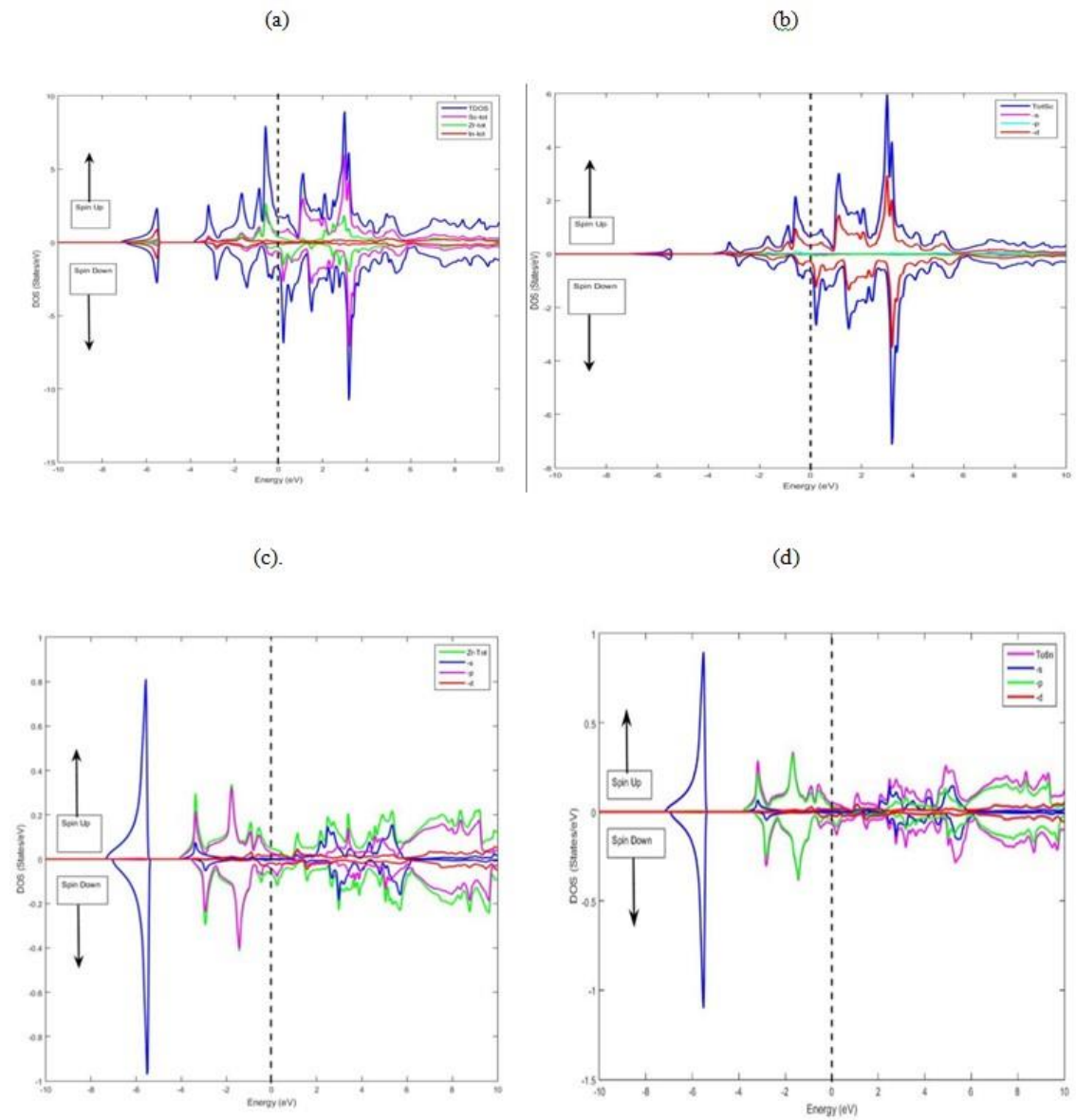


**Figure 21**

(a) Total density of states of spin up and spin down for inverse  $Sc_2ZrIn$  and partial density of states of spin up and spin down for (b) Sc1 atom (c) Sc2 atom (d) Zr atom (e) In atom of inverse compound using GGA method

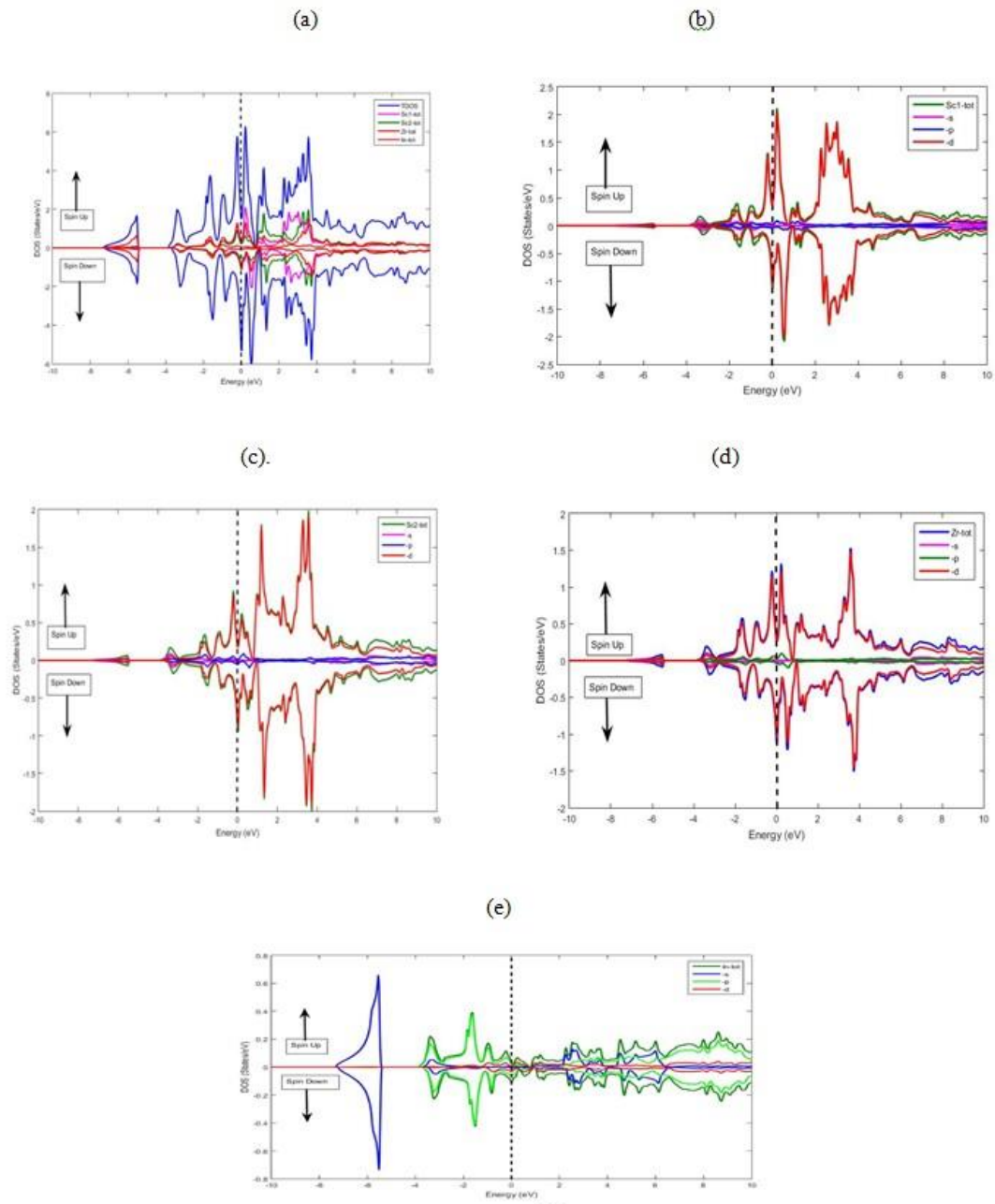
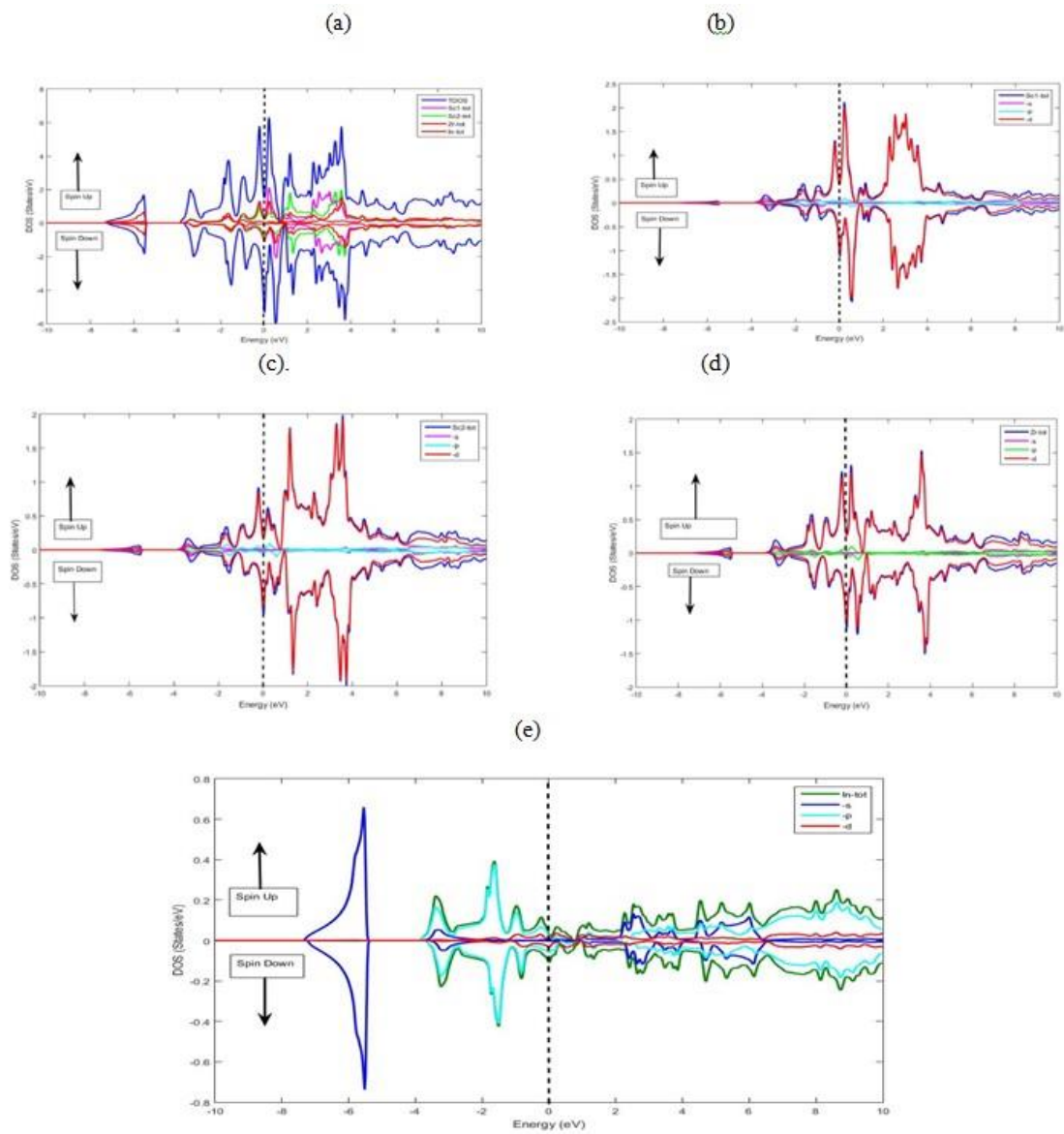


**Figure 22**

(a) Total density of states of spin up and spin down for inverse  $Sc_2ZrIn$  and partial density of states of spin up and spin down for (b) Sc1 atom (c) Sc2 atom (d) Zr atom (e) In atom of inverse compound using mBJ method





جامعة النجاح الوطنية  
كلية الدراسات العليا

الخصائص التركيبية، الالكترونية، المغناطيسية والمرونية لمركبات  
هزلة التامة  $Sc_2ZrIn$ ,  $Sc_2ZrAl$  باستخدام طريقة الجهد التام

إعداد

ربا زاهي ذيب الغرابة

إشراف

د. محمود الفاروط

أ. د. محمد أبو جعفر

قدمت هذه الرسالة استكمالاً لمتطلبات الحصول على درجة الماجستير في الفيزياء، من كلية الدراسات العليا، في

جامعة النجاح الوطنية، نابلس - فلسطين.

2024

الخصائص التركيبية، الالكترونية، المغناطيسية والمرونية لمركبات هزلة التامة  $Sc_2ZrAl$

$Sc_2ZrIn$ , باستخدام طريقة الجهد التام

إعداد

ربا زاهي ذيب الغرابة

إشراف

د. محمود الفاروط

أ. د. محمد أبو جعفر

### الملخص

تم دراسة الخصائص التركيبية، الالكترونية، المرونية، والمغناطيسية لمركبات هزلة التامة  $Sc_2ZrAl$  and  $Sc_2ZrIn$  باستخدام طريقة الجهد التام (FP-LAPW) والتي تعطي تقريبات أكثر دقة للتركيب الالكتروني للذرات. وكذلك تم استخدام نظرية الكثافة الوظيفية (DFT) والتي هي عبارة عن طريقة كمية حاسوبية تطبق ضمن اطار برنامج WIEN2k.

تم دراسة الخصائص التركيبية من خلال تطبيق التقريب التدريجي المعمم (GGA) بالإضافة الى استخدام نظام بيكي جونسون (mBJ) لتحسين النتائج في حسابات فجوة الطاقة. ميكانيكياً وجدنا أن المركبين في حالة normal أكثر استقراراً من inverse.

**الكلمات المفتاحية:** مركبات هزلة، مركبات هزلة التامة، التقريب التدريجي المعمم، نظام بيكي جونسون

اقتران الكثافة المحلية، الزخم المغناطيس.